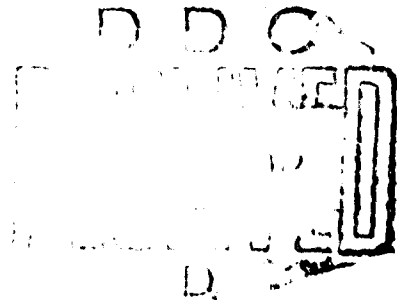AD743065

The Fast Field Program (FFP)
And Attenuation Loss in Hudson Bay

FREDERICK R. DiNAPOLI
MARY RITA POWERS
Computer Laboratory

19 April 1972

NAVAL UNDERWATER SYSTEMS CENTER

Approved for public release; distribution unlimited.

ADMINISTRATIVE INFORMATION

This research was conducted under NUSC Project No. A-670-10, "Acoustic Propagation Model for ASW Predictions," Principal Investigator, Dr. F. R. DiNapoli, Computer Laboratory (Code PA41), and Navy Subproject No. ZF XX 112 001, Program Manager, Dr. J. H. Huth (CNM DLP/MAT 03L4).

Portions of this report were presented orally as paper N6 at the 82nd Meeting of the Acoustical Society of America, Denver, Colorado, 20 October 1971.

The Technical Reviewer for this report was H. W. Marsh, Code CI.

REVIEWED AND APPROVED: 19 April 1972
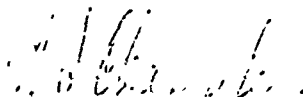
W. L. Clearvaters
Chief of Research and Development

ABSTRACT

The Fast Field Program (FFP) was developed to provide rapid, accurate, propagation-loss predictions for a generalized environmental model. This report demonstrates the utility of the FFP, in a different capacity, as a research tool to investigate the sound attenuation in a water column. Hudson Bay was selected as the area of application because the results of propagation experiments conducted there during August 1970 were available and interesting. The experimentally determined values of the attenuation coefficient for the frequency band 315 to 1600 Hz were found to exceed the values that would be predicted from existing formulas based on empirical relationships. The possibility that this anomalous behavior could have been due to energy leakage into the bottom is examined, and the values of the attenuation coefficient determined from the FFP analysis are compared with experimental results.

TABLE OF CONTENTS

LIST OF ILLUSTRATIONS

LIST OF ILLUSTRATIONS (Cont'd)

LIST OF TABLES

THE FAST FIELD PROGRAM (FFP)
AND ATTENUATION LOSS IN HUDSON BAY

INTRODUCTION

The increased interest, following World War II, in the propagation characteristics of lower frequency sound waves led to the discovery of two regimes of excess attenuation in sea water. The first occurred below 100 kHz, where the results of experiments conducted by numerous investigators[1] exhibited an increase in the attenuation coefficient of sea water over that of fresh water by a factor of approximately 20. This anomalous behavior was later identified with a relaxation process related to the $MgSO_4$ content of the sea water.

As the trend toward lower frequencies continued, a second anomaly was discovered, below 1 kHz. Although many explanations regarding the mechanism for this anomaly have been advanced, conclusive supporting evidence for any is lacking.

In 1965 Thorp[2] summarized the experimental results with the empirical formula

$$\alpha = \frac{.1 f^2}{1 + f^2} + \frac{40 f^2}{4100 + f^2} + 2.75 f^2 \times 10^{-4}. \tag{1}$$

The attenuation coefficient α is given in dB/kyd and the frequency f in kHz. The first term is identified with the unexplained anomaly below 1 kHz, the second with the $MgSO_4$ relaxation process, and the last with viscous absorption.

The analysis contained in this report is concerned with the appearance of a third regime of excess attenuation, for frequencies below 1 kHz, which was found in Hudson Bay.

SNYOPSIS OF THE EXPERIMENTAL RESULTS

In August of 1970, Browning et al.[3] conducted a long-range propagation experiment in Hudson Bay. The values of the attenuation coefficient determined from that experiment wore found to be considerably higher than the values that would be given by Eq. (1), Thorp's formula. A graphic comparison of the two results is provided in Fig. 1. Browning obtained his results by utilizing the assumed expression for propagation loss

$$N_w(f) = 10 \log R + H_0 + \frac{k}{f}R + \alpha_f R,$$

in which the terms are

$$\frac{\text{Total measured}}{\text{propagation loss}} = \text{Spreading loss} + \text{Channel leakage} + \text{Attenuation loss}.$$

The difference between the measured and assumed spreading losses was analyzed by means of linear regression. Assuming that leakage out of the channel was nugatory, the slope of the resulting regression line was set equal to α. It can be seen in Fig. 2, however, that the water depth over most of the tract was 600 feet, which results in an extremely weak sound channel. These facts lead to the conjecture that the low frequency anomaly shown in Fig. 1 may be due in part to the leakage of energy into the bottom. In order to gain additional insight into this aspect of the problem, the Fast Field Program (FFP) was utilized because both attenuation and bottom loss are incorporated into its transmission-loss predictions.

FFP FOR HUDSON BAY*

In Ref. 4 it is shown that, for a monochromatic point source at depth z_s, the field ψ, at some depth z and range r_n, is given by the discrete Fourier Transform:

$$\psi(z, r_n) \cong \Delta\xi \left(\frac{2}{\pi i}\right)^{1/2} \frac{e^{i\xi_0 r_n}}{r_n^{1/2}} \sum_{m=0}^{N-1} E_m \, e^{2\pi i m n/N}, \qquad (2)$$

where $n = 0, 1, \ldots, N-1$.

---

*Inasmuch as the analysis required in this section is an extension of the work reported in Ref. 4, only the essential aspects of the approach are noted here.

Equation (2) can be evaluated directly by means of the Fast Fourier Transform (FFT), which gives the value of the field at each of the N discrete ranges. The input to the FFT is found to be

$$E_m = G(z, z_s; \xi_m) \ \xi_m^{1/2} \ e^{imr_0\Delta\xi} , \tag{3}$$

where ξ_m is the discrete value of the horizontal component of the wave number, ξ_0 is the starting point in the sampled wave number space, and r_0 is the starting range value. The distance $\Delta\xi$ between samples in the wave number domain is related to the corresponding range sampling distance Δr by the relation

$$\Delta\xi = 2\pi/N\Delta r ,$$

where N, the order of the FFT, is 2 raised to some integer power.

The function G is the depth dependent Green's function, which must simultaneously satisfy both the differential equation

$$\frac{d^2\beta_j}{dz^2} + \left[\frac{\omega^2}{c_j^2(z)} - (\xi_m^2 - 2i\hat{\alpha}k_s) \right] \beta_j = 0 \quad z_j \le z \le z_{j+1} \tag{4}$$

and the associated boundary conditions. The value for k_s is arbitrarily determined from the depth of the source, and $\hat{\alpha}$ is the abbreviation for the attenuation coefficient in the water column in nepers/foot.

An efficient algorithm for the numerical evaluation of Eq. (3) results if the speed of sound is allowed to vary exponentially with depth within strata according to

$$c_j(z_i) = c_{j-1}(z_j) \ e^{\pm(z_i - z_j)/H_j} \quad z_j \le z_i \le z_{j+1} .$$

The solution of Eq. (4) is then found to be

$$\beta_j(z_i) = C_{\nu_j} [\gamma_j^i(z_i)] ;$$

that is, in terms of cylindrical functions of complex order,

$$\nu_j \cong [\xi_m H_j - i\hat{\alpha}H_j]$$

and the real argument is

$$\gamma_j^i(z_i) = \frac{\omega H_j}{c_{j-1}(z_j)} e^{\mp(z_i-z_j)/H_j} .$$

An excellent fit to the velocity profile shown in Fig. 2 is obtained by utilizing three strata having break points at the depths $z_2 = 52$, $z_j = 80$, and $z_4 = 600$ ft and having associated scale factors $H_1 = 8 \times 10^4$, $H_2 = -2 \times 10^3$, and $H_3 = 24 \times 10^4$.

The depth-dependent Green's function, $G(z, z_S; \xi_m)$, for the case in which the source and receiver are in the third layer is then given by

$$\frac{\dfrac{\pi H_3}{2}\left[\dfrac{H_3}{\gamma_3^4}Y_2^3 P_{\nu_3}(\gamma_3^3, \gamma_3^R) - R_{\nu_3}(\gamma_3^3, \gamma_3^R)\right]\left[Q_{\nu_3}(\gamma_3^S, \gamma_3^4) - \dfrac{i\omega\rho_w H_3}{\gamma_3^4}Y_4^4 P_{\nu_3}(\gamma_3^S, \gamma_3^4)\right]}{\dfrac{H_3}{\gamma_3^3}Y_2^3 Q_{\nu_3}(\gamma_3^3, \gamma_3^4) + \dfrac{i\omega\rho_w H_3}{\gamma_3^4}Y_4^4 R_{\nu_3}(\gamma_3^3, \gamma_3^4) - S_{\nu_3}(\gamma_3^3, \gamma_3^4) - i\omega\rho_w Y_2^2 Y_4^4 \dfrac{H_3 H_3}{\gamma_3^3 \gamma_3^4}P_{\nu_3}(\gamma_3^3, \gamma_3^4)}$$

$$z_3 \leq z \leq z_S ,$$

and

$$\frac{\dfrac{\pi H_3}{2}\left[\dfrac{H_3}{\gamma_3^4}Y_2^3 P_{\nu_3}(\gamma_3^3, \gamma_3^S) - R_{\nu_3}(\gamma_3^3, \gamma_3^S)\right]\left[Q_{\nu_3}(\gamma_3^R, \gamma_3^4) - \dfrac{i\omega\rho_w H_3}{\gamma_3^4}Y_4^4 P_{\nu_3}(\gamma_3^R, \gamma_3^4)\right]}{\dfrac{H_3}{\gamma_3^3}Y_2^3 Q_{\nu_3}(\gamma_3^3, \gamma_3^4) + \dfrac{i\omega\rho_w H_3}{\gamma_3^4}Y_4^4 R_{\nu_3}(\gamma_3^3, \gamma_3^4) - S_{\nu_3}(\gamma_3^3, \gamma_3^4) - i\omega\rho_w Y_2^2 Y_4^4 \dfrac{H_3 H_3}{\gamma_3^3 \gamma_3^4}P_{\nu_3}(\gamma_3^3, \gamma_3^4)}$$

$$z_S \leq z \leq z_4 ,$$

4

where the admittance of the first layer evaluated at z_2 is given by

$$Y_1^2 = \frac{\gamma_1^2}{H_1} \frac{Q_{\nu_1}(\gamma_1^1, \gamma_1^2)^*}{P_{\nu_1}(\gamma_1^1, \gamma_1^2)}$$

and the admittance of the second layer at z_2 is found, from the continuity conditions, to be

$$Y_2^3 = \frac{\gamma_2^3}{H_2} \frac{\left| \dfrac{H_2}{\gamma_2^2} Y_1^2 Q_{\nu_2}(\gamma_2^2, \gamma_2^3) - S_{\nu_2}(\gamma_2^2, \gamma_2^3) \right|}{\left| \dfrac{H_2}{\gamma_2^2} Y_1^2 P_{\nu_2}(\gamma_2^2, \gamma_2^3) - R_{\nu_2}(\gamma_2^2, \gamma_2^3) \right|}.$$

The bottom is assumed to consist of M fluid layers, each having a constant velocity and constant density. The admittance that the bottom presents to the water column is then found to be[5]

$$Y_j^j = K_j \frac{\left[Y_{j+1}^{j+1} - K_j \tanh(\Lambda_j) \right]}{\left[K_j - Y_{j+1}^{j+1} \tanh(\Lambda_j) \right]},$$

where $j = 4, 5, \ldots, M+4$, and the argument of the hyperbolic function is

$$\Lambda_j = id_j (k_z)_j$$

with d_j denoting the thickness of the j-th layer. The vertical component of the wave number is abbreviated as

$$(k_z)_j = \sqrt{k_j^2 - \xi_m^2 + 2i \hat{\alpha}_B k_j},$$

---

*The definition of the products of cylindrical functions is given by Ref. 4, Eq. (11).

and the characteristic plane wave admittance is abbreviated as

$$K_j = (k_z)_j / \omega \rho_j \, ,$$

where k_j and ρ_j represent the wave number and density, respectively, in the bottom layer.

The attenuation in each bottom layer was arbitrarily set equal to the same parameter $\hat{\alpha}_B$ for convenience.

ENERGY LEAKAGE INTO THE BOTTOM

Determination of whether or not energy leakage into the bottom had a significant effect* on acoustic propagation for frequencies above 315 Hz[†] in Hudson Bay is hampered by the lack of bottom-loss information for the desired frequency range — a lack not uncommon to determinations of this type. Therefore, the approach utilized was to fix the value of attenuation in water at some reasonable value and allow the bottom admittance Y_4^4 to vary, which was accomplished by changing the velocity, density, attenuation, or layer thickness of the subbottom strata.

Inasmuch as the limited bottom information available suggested a layer of mud overlying bedrock, the primary model was assumed to consist of two fluid layers. This model admits the phenomena associated with intromission and total reflection, and it yields a frequency-dependent bottom loss. A core analysis would certainly show considerably more stratification than could be accommodated by two layers, but the total bottom loss may be substantially the same for either case due to frequency dependence. The assumed bottom-loss model is not a complete representation of the detailed subbottom structure, but it is felt to be adequate for evaluating the effect of energy leakage into the bottom.

The parameters describing the bottom were varied to produce substantially different bottom-loss cases. The resulting FFP transmission-loss estimates were then examined for salient differences. This process was

---

*For this study, a "significant" effect means one that alters the slope of the analytical propagation-loss prediction curve.

[†]315 Hz was selected as the low-frequency limit because no experimental data for lower frequencies were available.

started at 315 Hz and repeated for additional higher frequencies. For frequencies 315 Hz or higher, the influence of the bottom could only be detected at close range. A typical example of this analysis is provided in Fig. 3. An examination of the associated bottom parameters listed in Table 1 reveals that the layers are identical except for the values of bottom attenuation, but the difference is sufficient to cause the bottom-loss values shown in Fig. 3A. Case A is a very-low-loss bottom, and an average of about 6 dB loss is found for case B. The propagation-loss predictions for both cases have been superimposed to facilitate visual comparison. It is seen that beyond 10 kyd the two results are practically indistinguishable; there were no significant effects of bottom influence for the higher frequencies investigated.

The same procedure was then repeated for progressively lower frequencies below 315 Hz. As expected, the influence of the bottom gradually became more pronounced as frequency decreased. It is apparent in Fig. 4 (Table 2 refers) that at 100 Hz the bottom has a more pronounced influence at longer ranges than was found at 315 Hz; this same bottom structure results in a significantly different transmission loss prediction at 50 Hz. Figure 5 (Table 3 refers) shows typical effects of changing bottom parameters at 50 Hz. It is evident from these cases that, even if experimental data were available below 315 Hz, it would be very difficult to make a determination regarding attenuation without detailed subbottom information. The assumption of a fluid bottom would also be suspect at lower frequencies because it could not account for the transverse waves that exist in a solid bottom. It is felt that in the frequency region about 315 Hz, however, bottom types were examined in sufficient variety to conclude that energy leakage does not have a significant effect in the determination of attenuation coefficients.

ATTENUATION IN THE WATER COLUMN

The attenuation coefficient was determined by finding a value that produced a close comparison between transmission losses (at each frequency) of the FFP predictions and the experimental data. However, before the results of the comparative process are discussed, it is worth noting the essentially different elements of the two sets of data.

The distance between the experimental data points was 3 nautical miles, whereas the corresponding distance for the FFP was about 50 yards. The FFP thus shows the interference pattern in considerably more detail than the experimental data.

Table 1

BOTTOM PARAMETERS AT 315 Hz

Case	Layer	Velocity (ft/sec)	Attenuation (dB/ft)	Layer Thickness (ft)	Density Ratios
A	1	5,000	0.4	10	$\rho_1/\rho_w = 1.5$
	2	12,000	0.4	∞	$\rho_1/\rho_2 = 0.077$
B	1	5,000	0.0	10	$\rho_1/\rho_w = 1.5$
	2	12,000	0.0	∞	$\rho_1/\rho_2 = 0.077$

Table 2

BOTTOM PARAMETERS AT 100 Hz

Case	Layer	Velocity (ft/sec)	Attenuation (dB/ft)	Layer Thickness (ft)	Density Ratios
A	1	5,000	0.0	10	$\rho_1/\rho_w = 1.5$
	2	12,000	0.0	∞	$\rho_1/\rho_2 = 0.077$
B	1	5,000	0.0	100	$\rho_1/\rho_w = 1.5$
	2	12,000	0.0	∞	$\rho_1/\rho_2 = 0.077$

Table 3

BOTTOM PARAMETERS AT 50 Hz

Case	Layer	Velocity (ft/sec)	Attenuation (dB/ft)	Layer Thickness (ft)	Density Ratios
A	1	5,000	0.0	10	$\rho_1/\rho_w = 1.5$
	2	12,000	0.0	∞	$\rho_1/\rho_2 = 0.077$
B	1	5,000	0.0	10	$\rho_1/\rho_w = 1.5$
	2	8,000	0.0	∞	$\rho_1/\rho_2 = 0.077$

It was originally thought that it would be helpful in comparing the results if, having removed the trend of 10 log R, the analytical values were fitted by a linear regression analysis. As the frequency increases so does the number of allowable modes and a greater fluctuation in the transmission-loss values results; the regression analysis should then be most useful at the higher frequencies. An example of this analysis is provided in Fig. 6 at a frequency of 1000 Hz. Although considerable fluctuation is evident, the overall slope of the FFP curve is well behaved, as evidenced by the fact that input value for the attenuation coefficient agrees to the first two decimal places with the slope of the regression line. It was therefore decided that a subjective comparison could be satisfactorily accomplished without the need for regression analysis.

Another consideration was the comparison of single-frequency FFP estimations with the 1/3-octave averages of the bomb-shot data. In Figs. 7 and 8, the FFP results are plotted for the end-point frequencies of the 1/3-octave band about 1000 Hz. The predictions at the center frequency and the average of the three cases are shown in Figs. 9 and 10, respectively. As might be expected, the averaged result shows less fluctuation than any of its components. It is also evident that the slopes of the curves in Figs. 9 and 10 are in good agreement. Inasmuch as the 1/3-octave bandwidths diminish with decreasing frequency, it was decided that a center-frequency prediction would be adequate for this analysis.

The last consideration was the effect of a change in the input value of attenuation on the FFP transmission-loss predictions. Although it would be mathematically correct to utilize a complex wave number, in normal mode calculations the wave number is usually assumed to be a real valued function. Attenuation is then accounted for through the ancillary term αr with r being the horizontal distance. The introduction of an attenuation loss into theoretic ray calculations can be accomplished either in the same fashion or by accounting for the loss along the ray paths.[6] The wave number is assumed to be complex in the FFP analysis, and the αr term is not used in computing transmission loss. From the viewpoint of normal mode theory, this would be equivalent to rotating the singularities away from the axis of integration, thereby causing each mode to be attenuated by a different amount. In Fig. 11, the FFP transmission-loss values are plotted, using three different input values for the attenuation coefficient for a frequency of 315 Hz. Except for the noticeable sharpening of the mode interference pattern, the difference in slope between each of the cases is proportional to the difference in attenuation values. This happy state of affairs will not persist, however, for an excessive ratio of the input values for α, such as approximately 20 to 1.[7] Accounting for attenuation on the basis of path length in ray calculations should produce substantially

the same result as the αr term for the source and receiver on the axis of minimum velocity of sound. The greatest deviation between the horizontal separation of source and receiver and the path length would be for high-angle rays, and the spreading loss associated with these rays would be generally greater than that of the nearly axial rays.

In comparing the FFP with the bomb-shot data, the input value of the attenuation coefficient ultimately selected was that value which allowed the experimental results to bisect the FFP interference pattern. This procedure was repeated for each center frequency, and the comparisons are shown in Figs. 12 through 19. The variations in both experimental data and FFP predictions introduce some uncertainties in subjectively selecting the best fits. This is readily evident in Fig. 20, where the transmission losses for two slightly different input values of attenuation are plotted against the bomb-shot data. An effort was made to determine the minimum and maximum values of α which could be used and still produce a reasonable fit. The result of this judgment is represented by the dashed lines in Fig. 21; the dots within the envelope are the values considered to produce the best comparison with the experimental data. Finally, in Fig. 22, Browning's initial estimates of the excess attenuation in Hudson Bay are compared with the values determined by FFP analysis. The agreement between the two is quite good, except at the lowest frequencies where Browning's values show a trend towards higher values of attenuation.

<div align="center">DISCUSSION</div>

The results of this analytical study agree with Browning's initial estimates of excess attenuation in Hudson Bay. Since the attenuation is excess with reference to Thorp's formula, it is worth noting that the data used by Thorp were mostly from deep water, whereas Hudson Bay would have to be considered shallow by comparison. Furthermore, Hudson Bay is relatively cold and low in salt content (surface salinity 26 parts per thousand). When the attenuation values from Hudson Bay are compared with those from a more closely related environment, as shown in Fig. 23 for the values Marsh and Elam* found for the Gulf of Maine, both are found to exceed Thorp's reference by about the same amount. In order to determine if this anomaly is unique ' ' shallow water, an additional experiment is planned for Baffin Bay, which is cold water but considerably deeper than either the Gulf of Maine or Hudson Bay.

*Personal communication with H. W. Marsh, 1971.

REFERENCES

1. W. H. Thorp et al., "A Review of Low Frequency Sound Attenuation in the Ocean," presented as paper Y1 at the Eighty-first Meeting of the Acoustical Society of America, Washington, D. C., 20-23 April 1971.

2. W. H. Thorp, "Deep Ocean Sound Attenuation in the Sub and Low Kilocycle per Second Region," Journal of the Acoustical Society of America, vol. 38, no. 4, October 1965, pp. 648-654.

3. D. G. Browning et al., Project CANUS: Sound Propagation and Reverberation Measurements in Hudson Bay, NUSC Report No. 4221, 1 December 1971.

4. F. R. DiNapoli, Fast Field Program for Multilayered Media, NUSC Report No. 4103, 26 August 1971.

5. L. M. Brekhovskikh, Waves in Layered Media, Academic Press, New York, 1960, p. 59.

6. H. Weinberg, CONGRATS I: Ray Plotting and Eigenray Generation, NUSL Report No. 1052, 30 October 1969, p. 6.

7. F. R. DiNapoli, Acoustic Propagation in a Stratified Medium, NUSL Report No. 1046, 13 August 1969, Fig. 15.
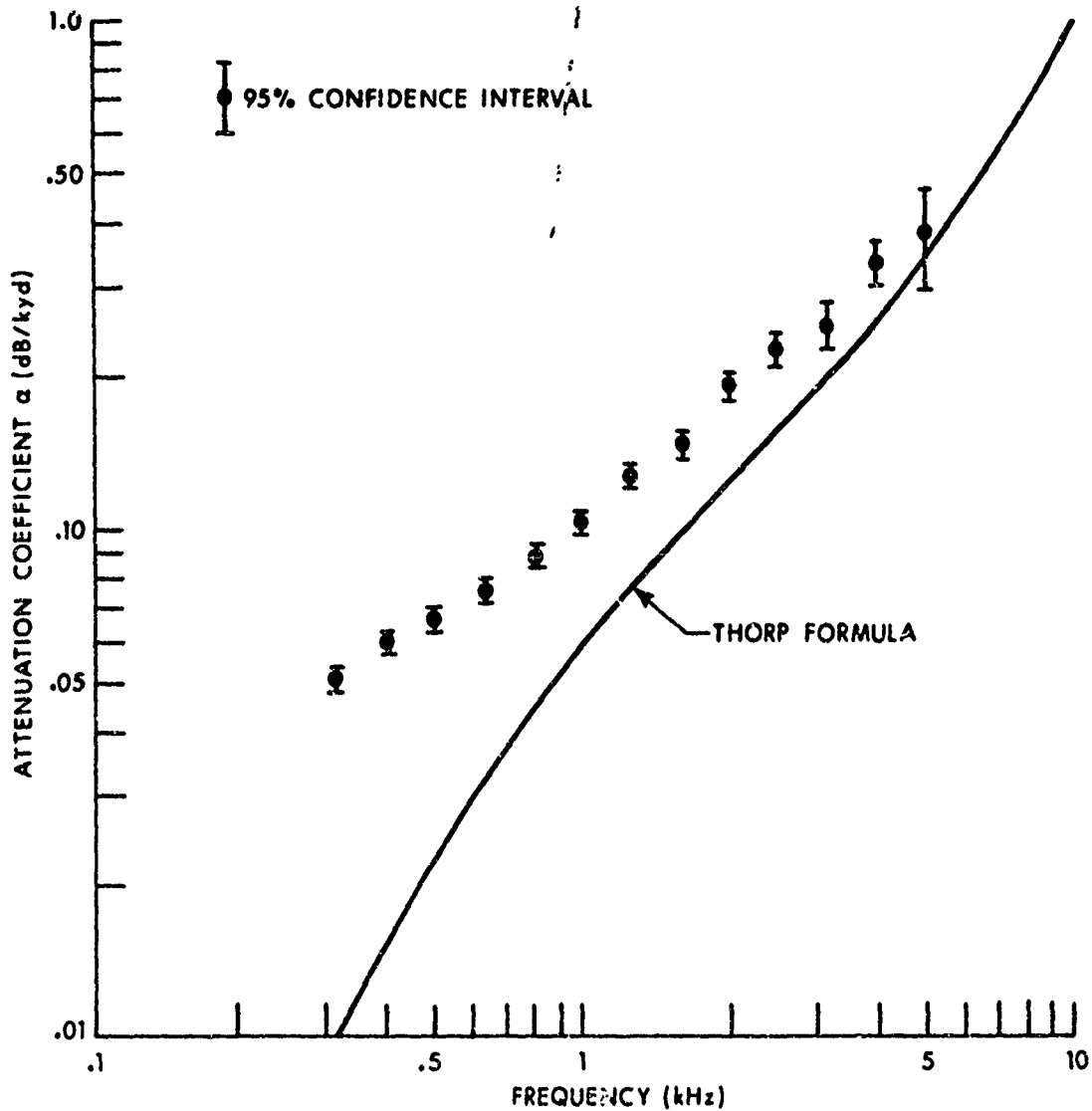
Fig. 1. Comparison of Attenuation Coefficients for Thorp's Formula
and for Hudson Bay Experimental Results
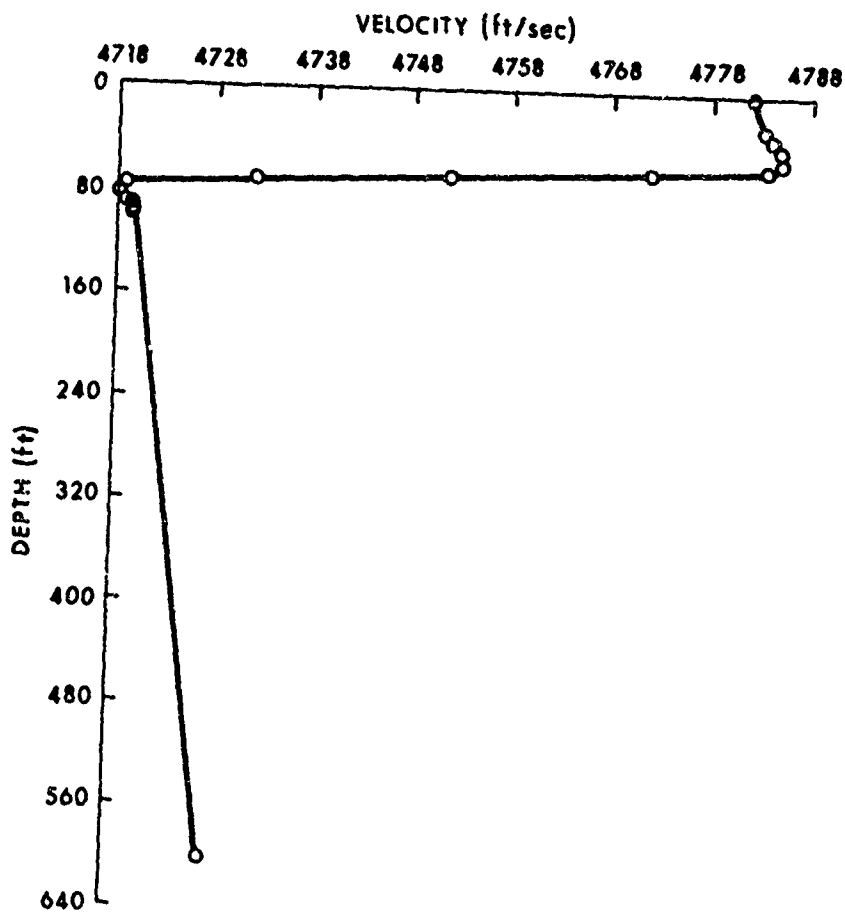
Fig. 2A. Velocity Profile
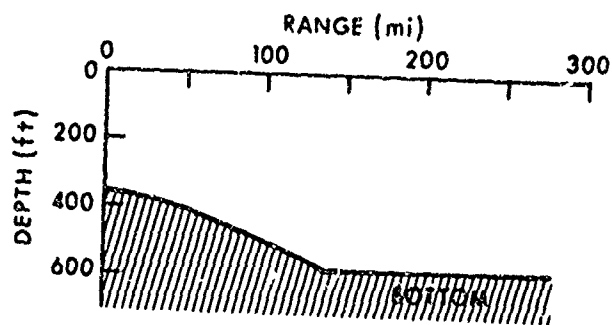
Fig. 2B. Depth Profile

Fig. 2. Acoustic Environment of Hudson Bay (15 August 1970)
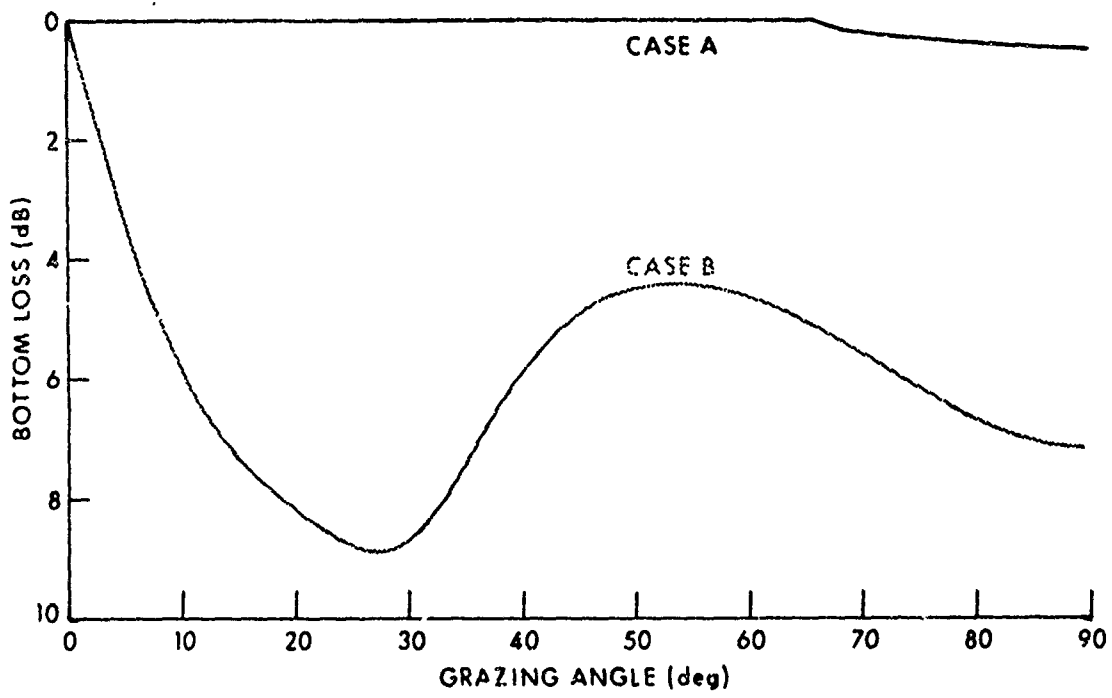
Fig. 3A. Bottom Losses
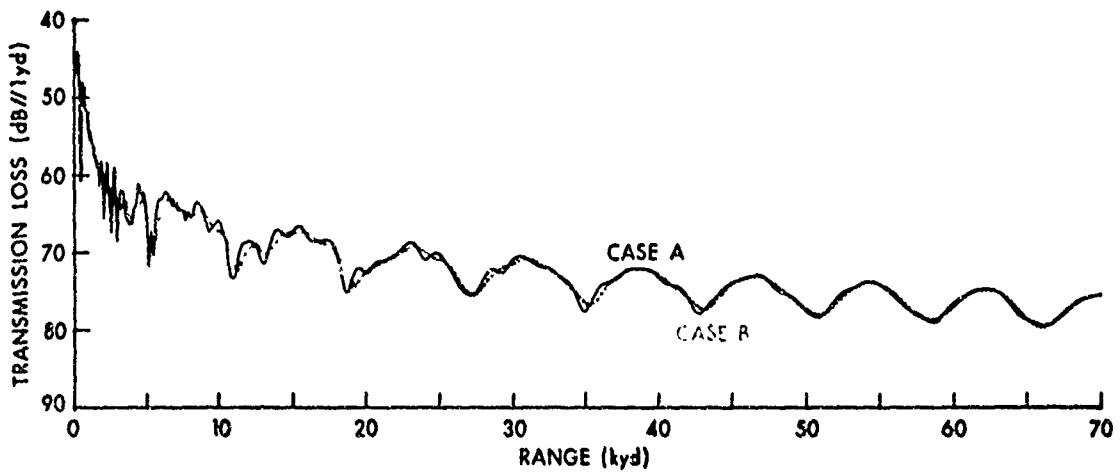
Fig. 3B. Transmission Losses

Fig. 3. Effect of Various Bottom Attenuations on Transmission Losses at 315 Hz
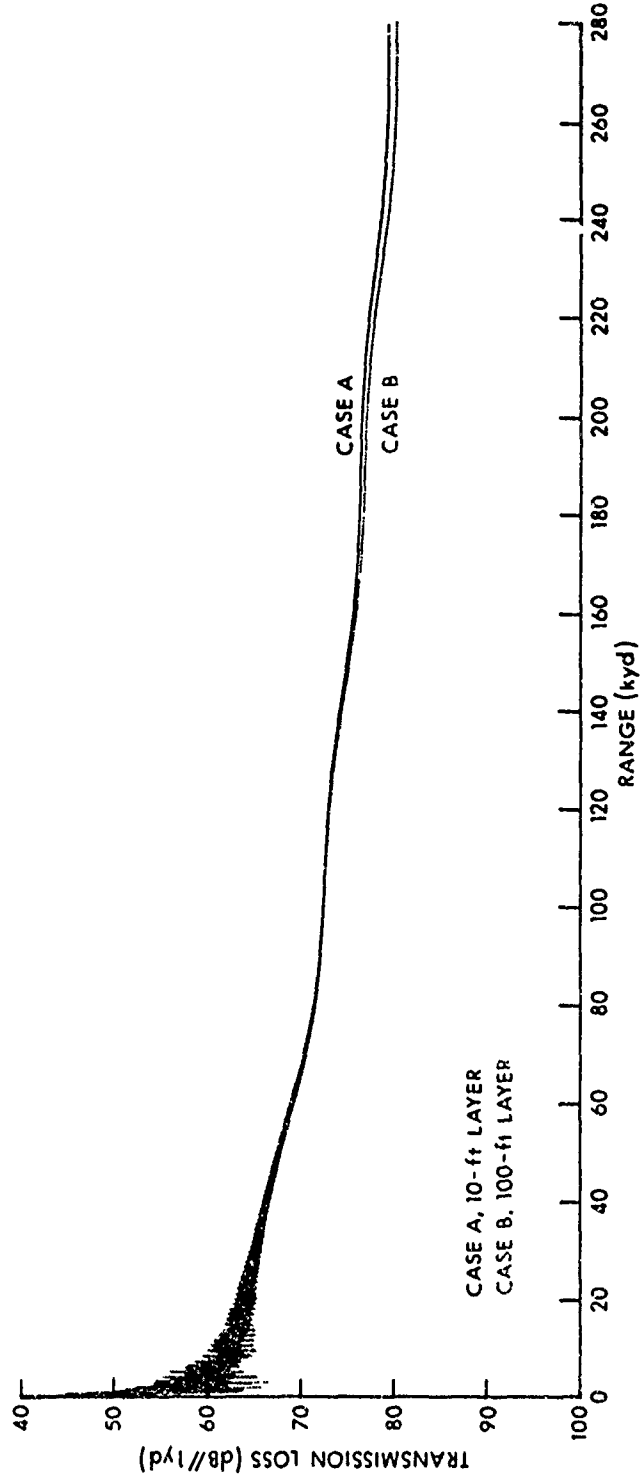
Fig. 4. Effect of Various Bottom Layer Thicknesses on Transmission Losses at 100 Hz
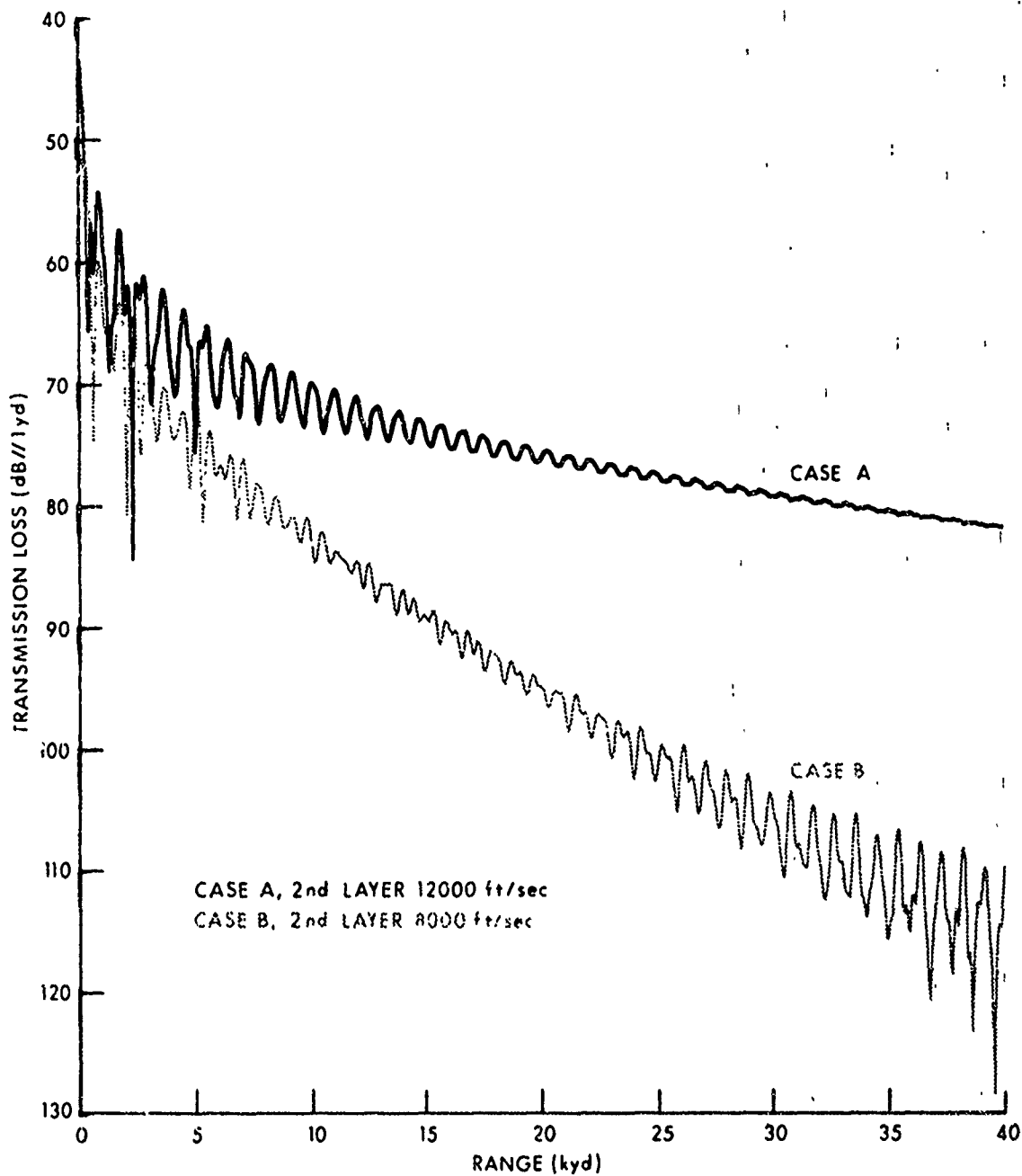
Fig. 5. Effect of Various Bottom Layer Velocities on Transmission Losses at 50 Hz
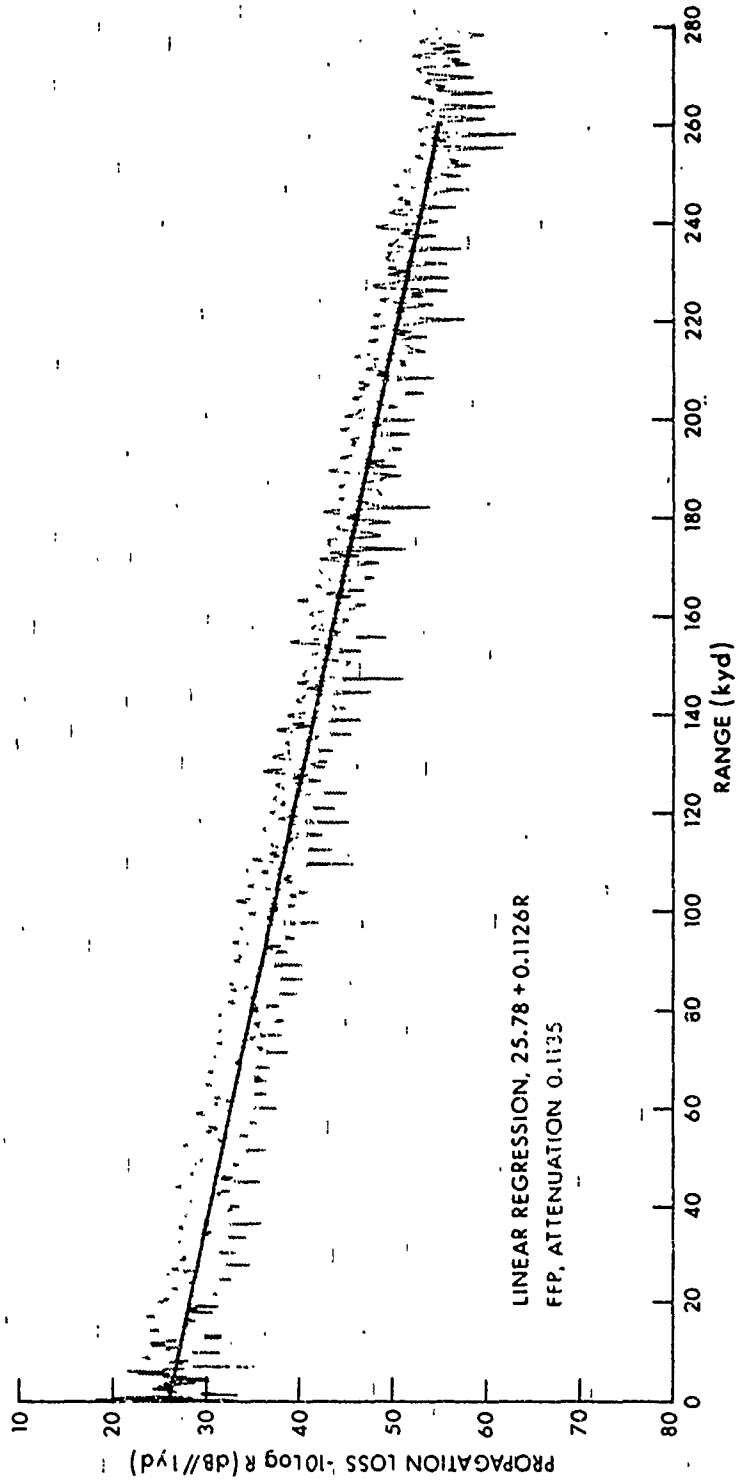
Fig. 6. Regression Analysis at 1000 Hz

LINEAR REGRESSION, 25.78 + 0.1126R

FFP, ATTENUATION 0.1135
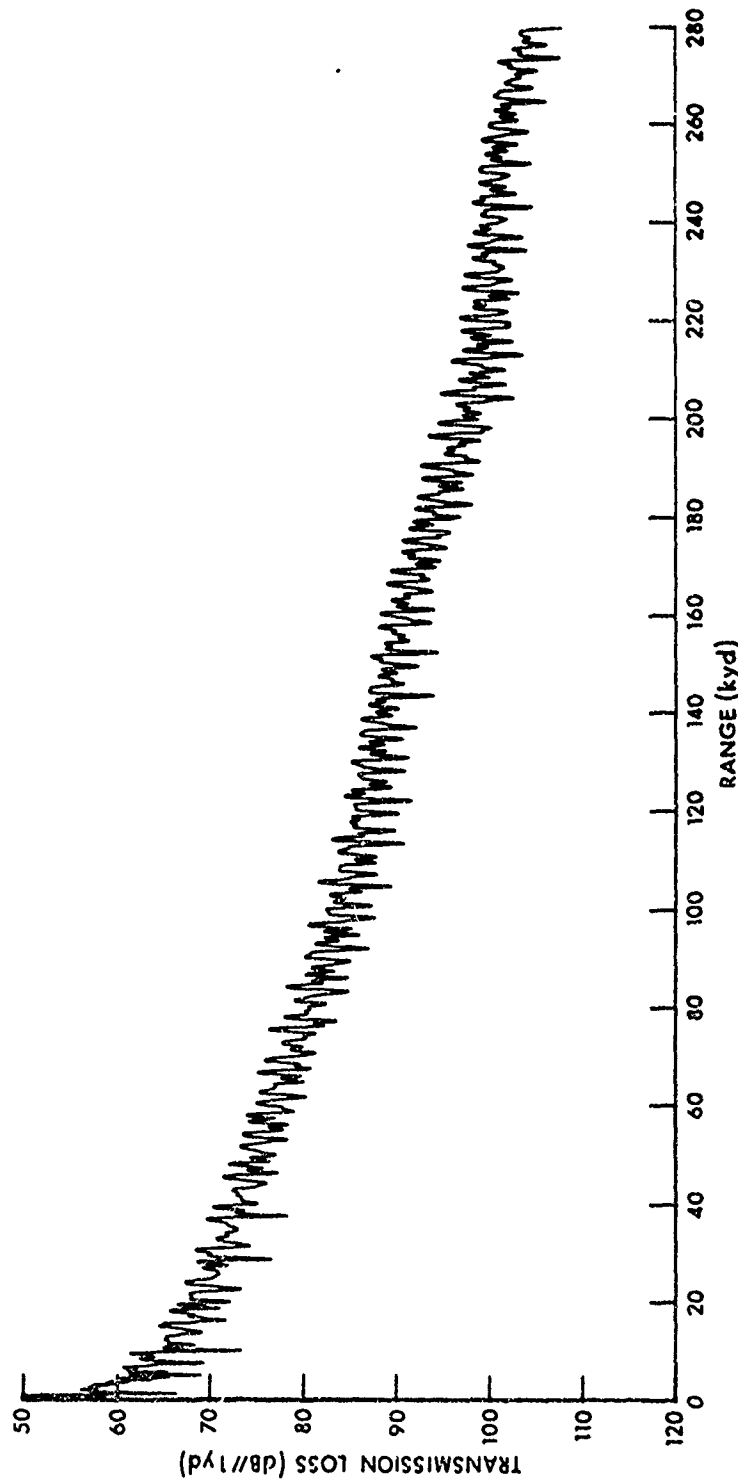
Fig. 7. FFP Transmission Loss at 894 Hz
(Attenuation = $1.9\,\alpha_{Thorp}$)
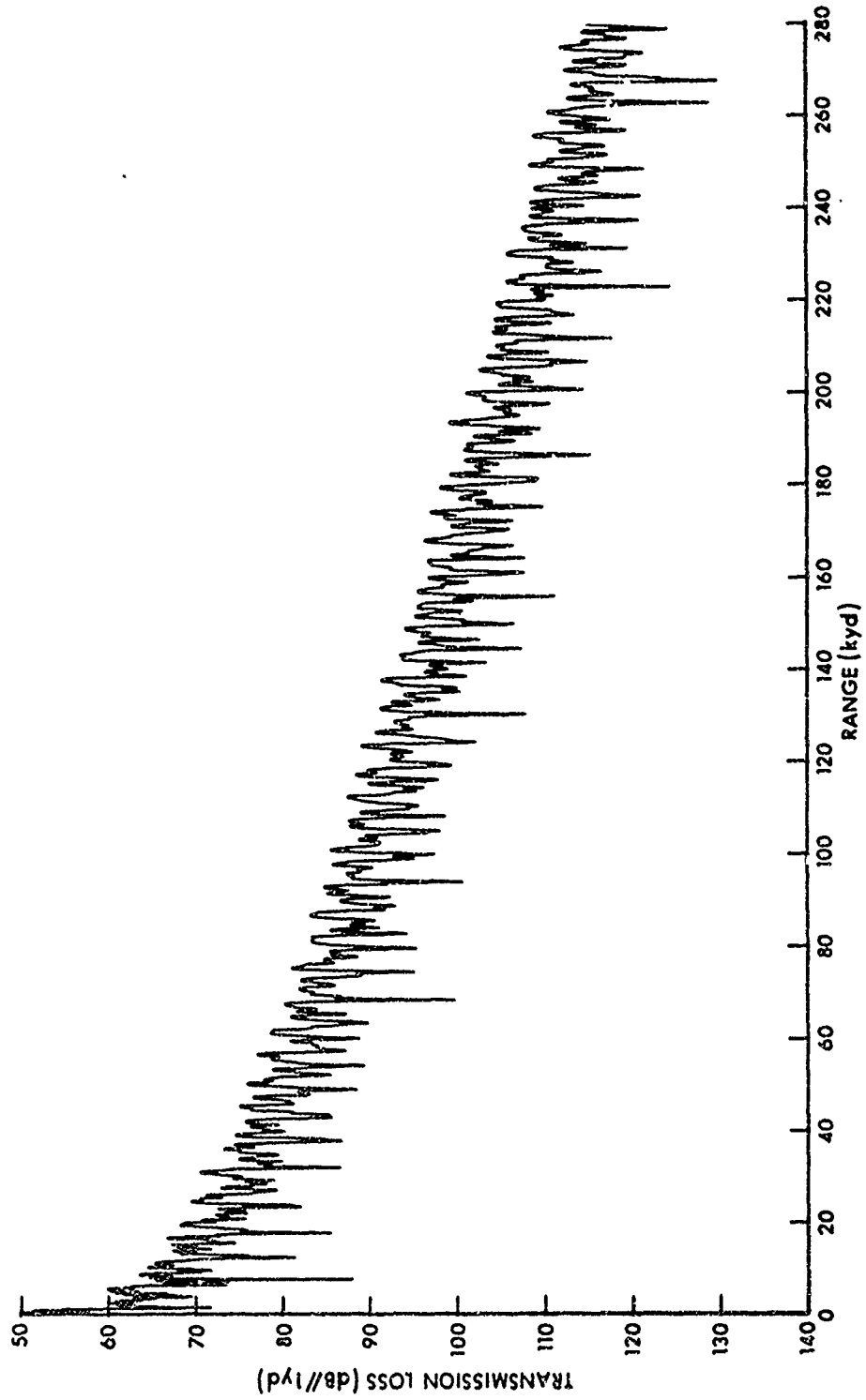
Fig. 8. FFP Transmission Loss at 1118 Hz
(Attenuation = 1.9 α_{Thorp})
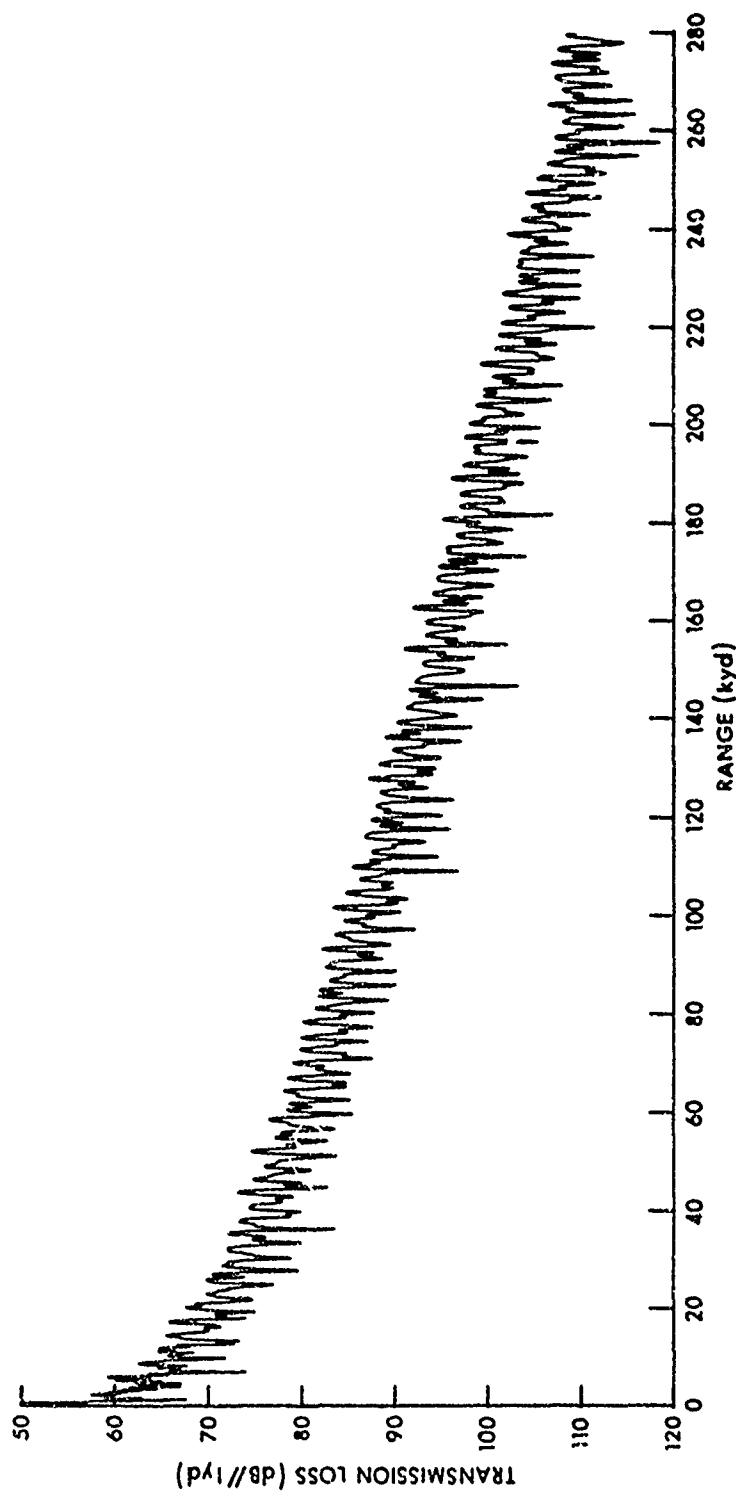
Fig. 9. FFP Transmission Loss at 1000 Hz
(Attenuation = $1.9\, a_{Thorp}$)
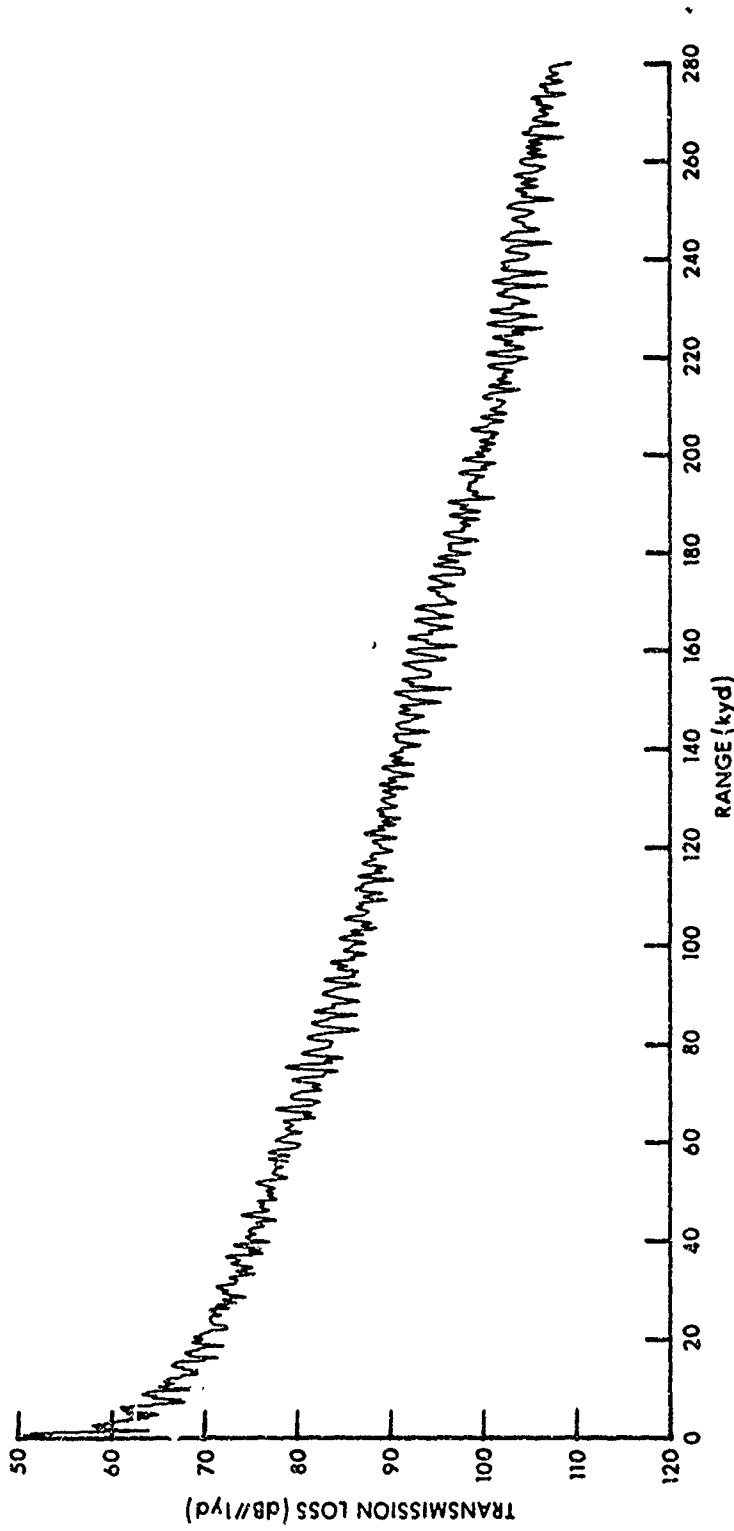
Fig. 10. FFP Transmission Loss, 1/3-Octave Average About 1000 Hz
(Attenuation = $1.9 \, a_{Thorp}$)
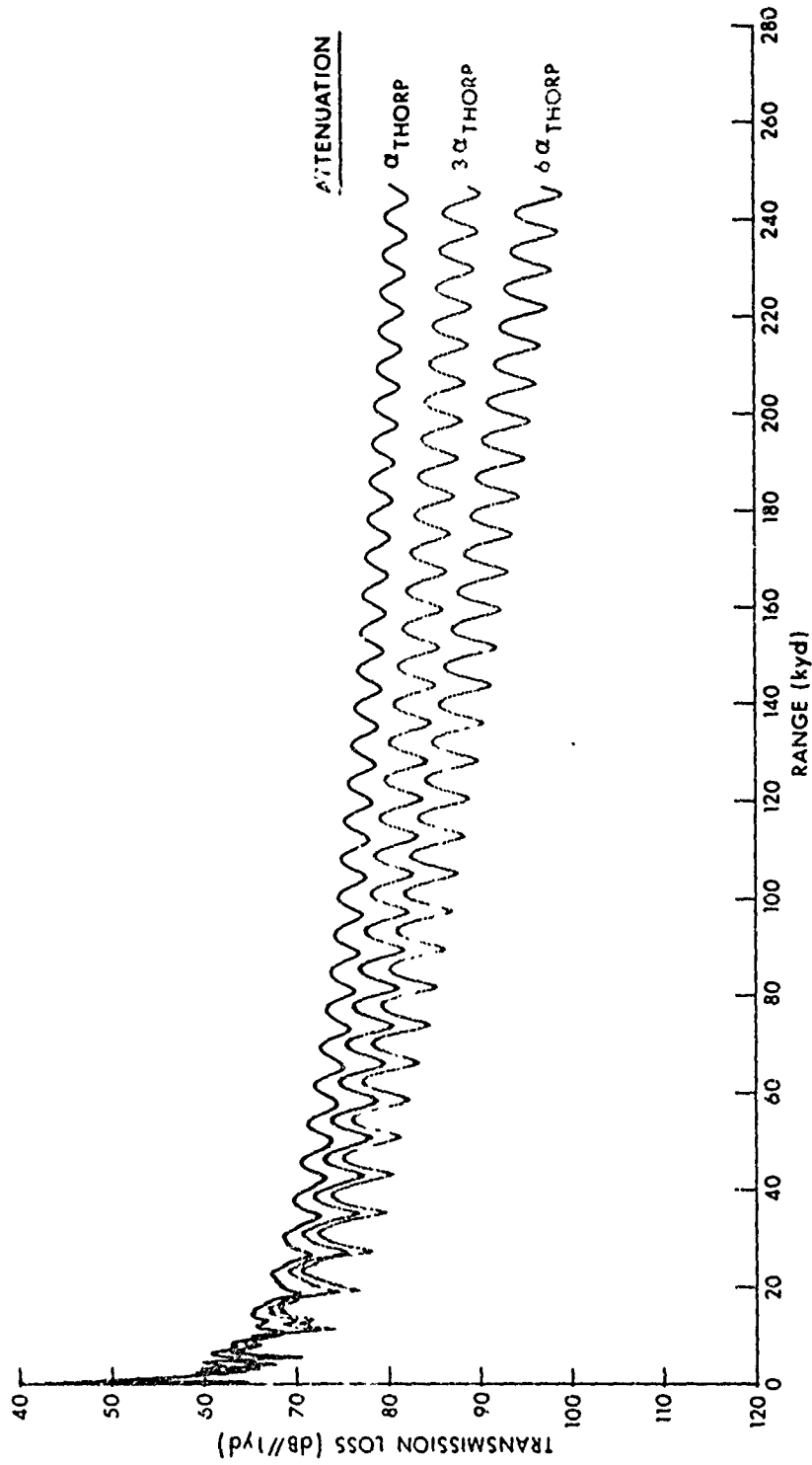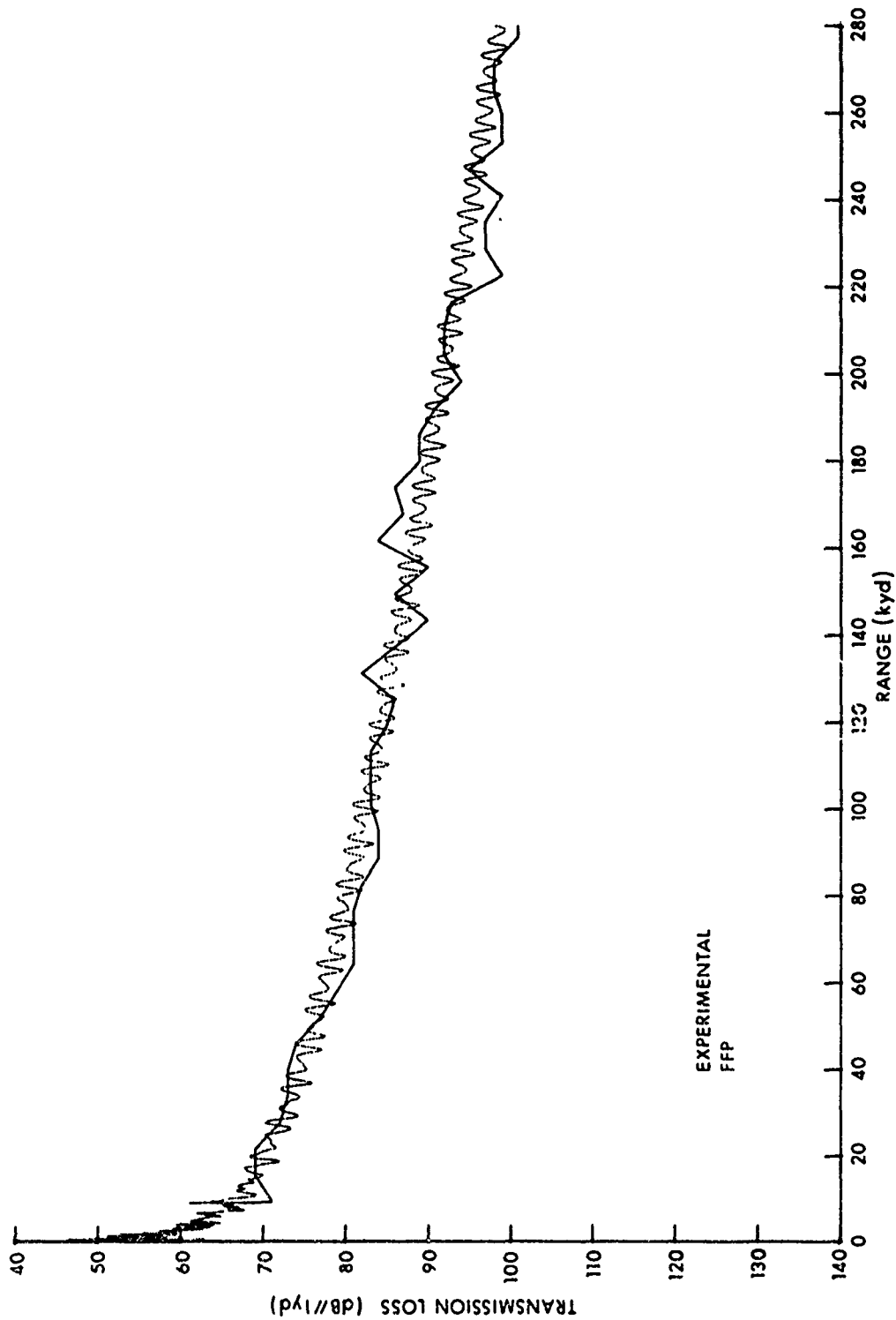
Fig. 11. Effect of Attenuation on FFP Transmission Loss
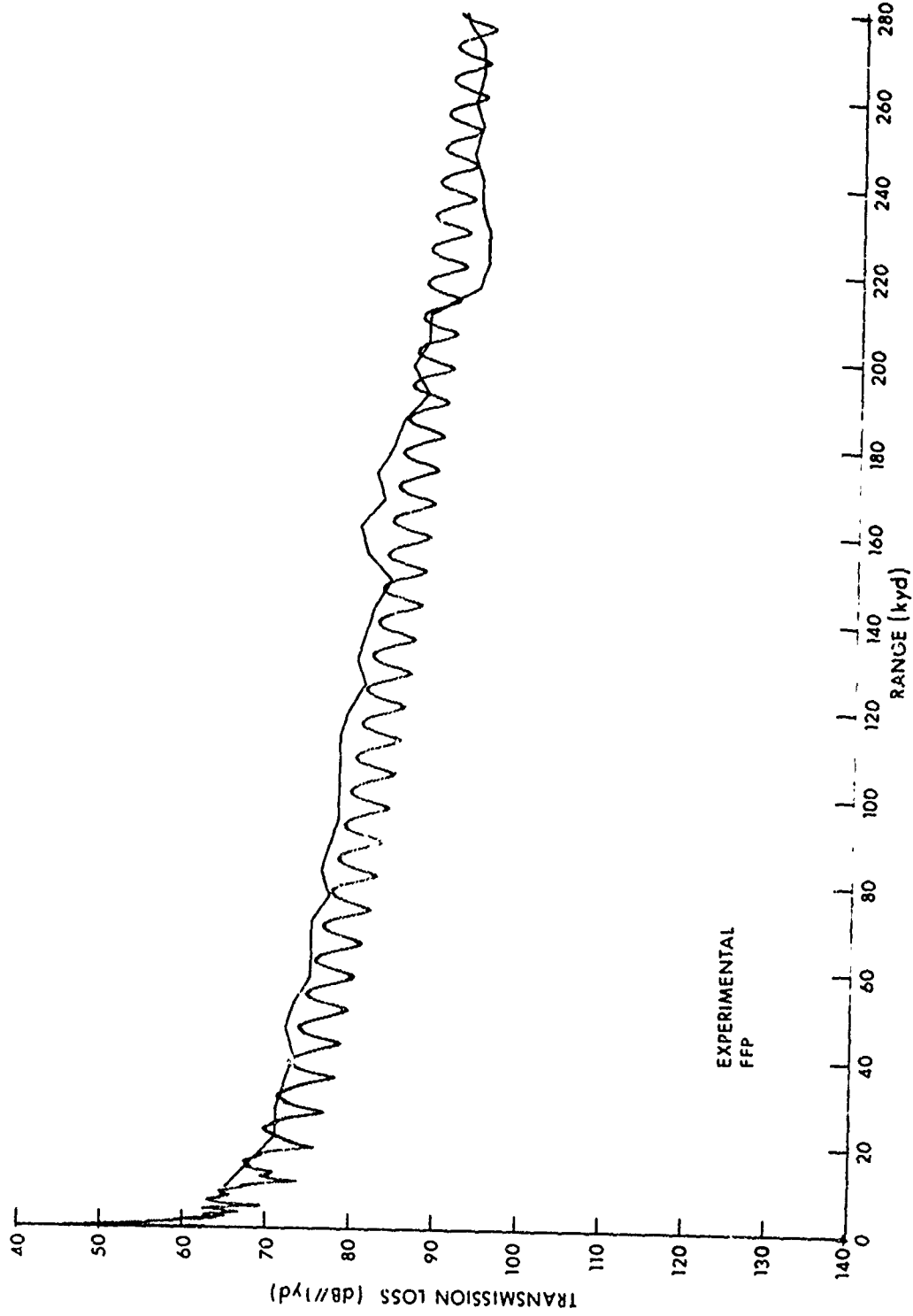
Fig. 12. FFP and Hudson Bay Experimental Transmission Losses at 315 Hz
(Source Depth 175 ft, Receiver Depth 175 ft, Attenuation 0.0400 dB/kyd)
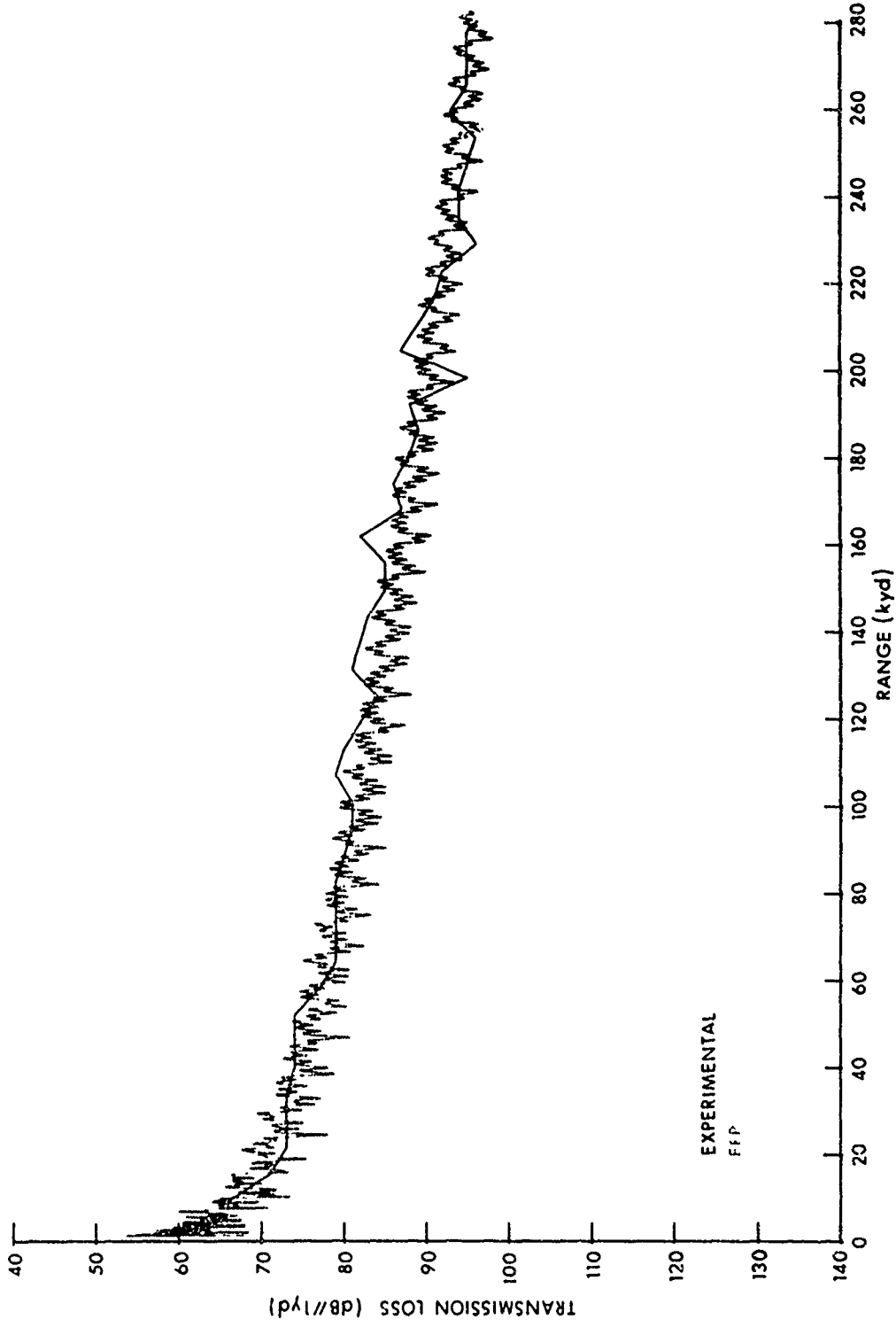
Fig. 13. FFP and Hudson Bay Experimental Transmission Losses at 400 Hz
(Source Depth 175 ft, Receiver Depth 175 ft, Attenuation 0.0537 dB/kyd)
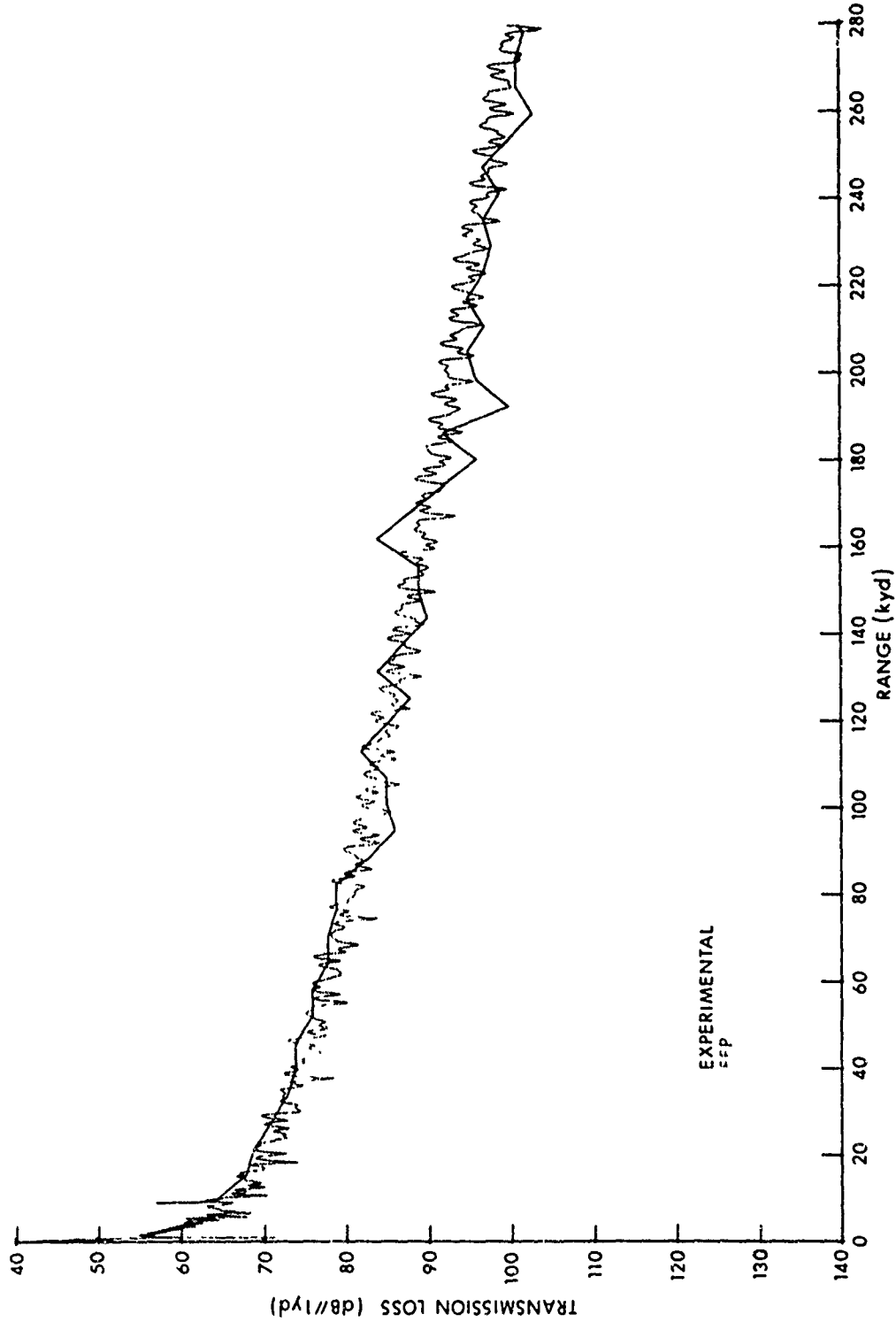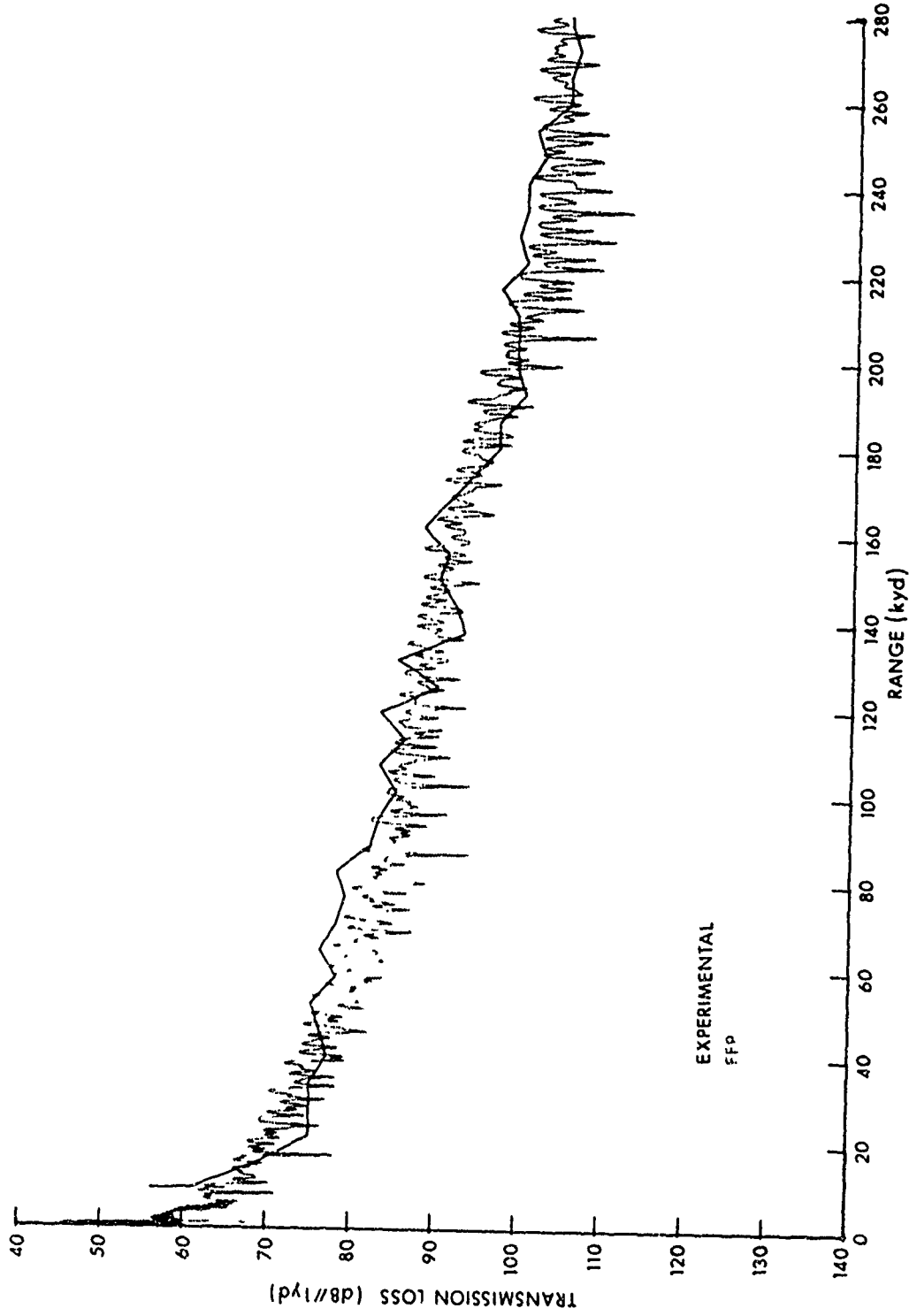
Fig. 14. FFP and Hudson Bay Experimental Transmission Losses at 500 Hz
(Source Depth 175 ft, Receiver Depth 175 ft, Attenuation 0.0640 dB/kyd)

Fig. 15. FFP and Hudson Bay Experimental Transmission Losses at 630 Hz
(Source Depth 175 ft, Receiver Depth 175 ft, Attenuation 0.0719 dB/kyd)

Fig. 16. FFP and Hudson Bay Experimental Transmission Losses at 800 Hz
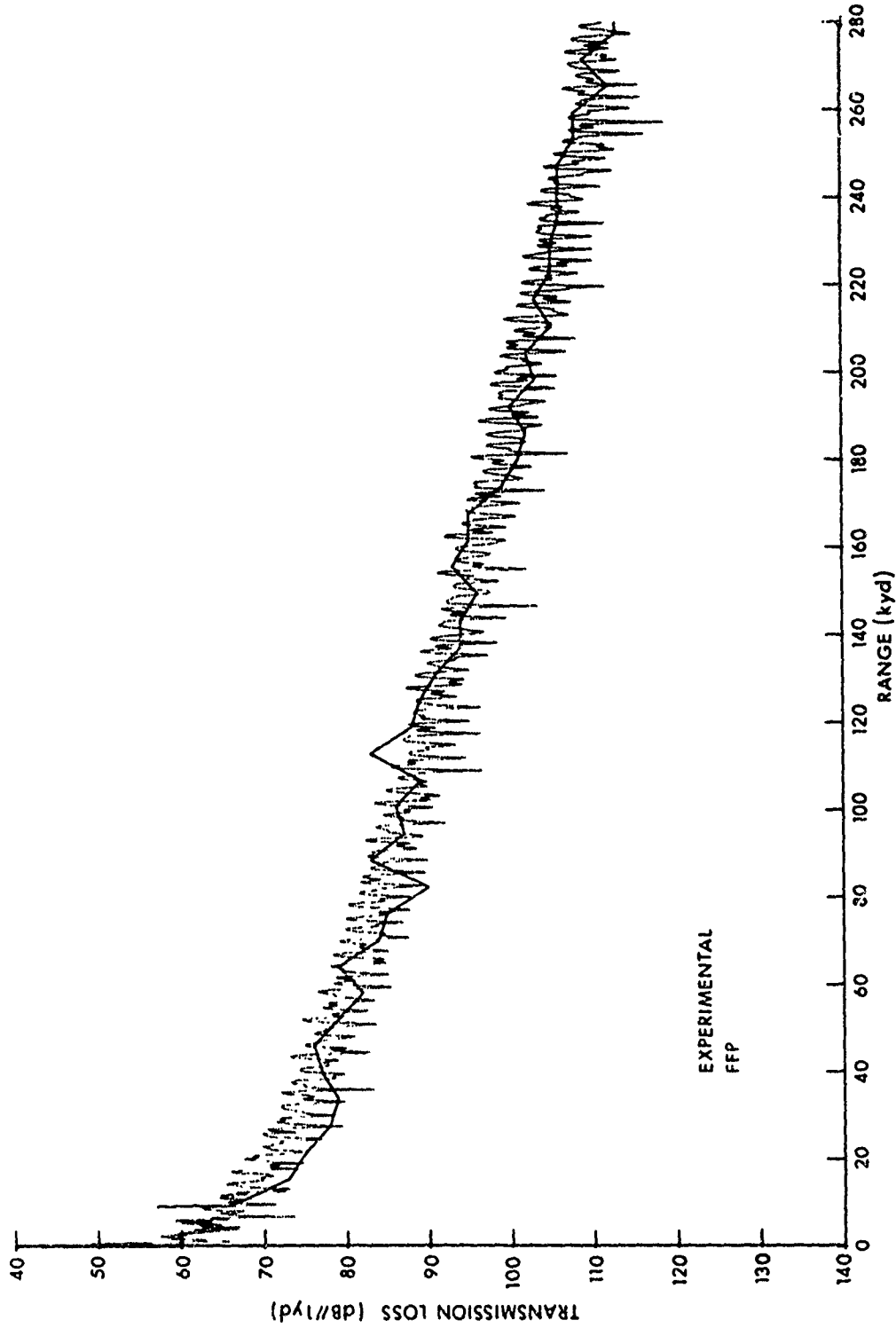(Source Depth 175 ft, Receiver Depth 175 ft, Attenuation 0.0905 dB/kyd)

Fig. 17. FFP and Hudson Bay Experimental Transmission Losses at 1000 Hz (Source Depth 175 ft, Receiver Depth 175 ft, Attenuation 0.114 dB/kyd)
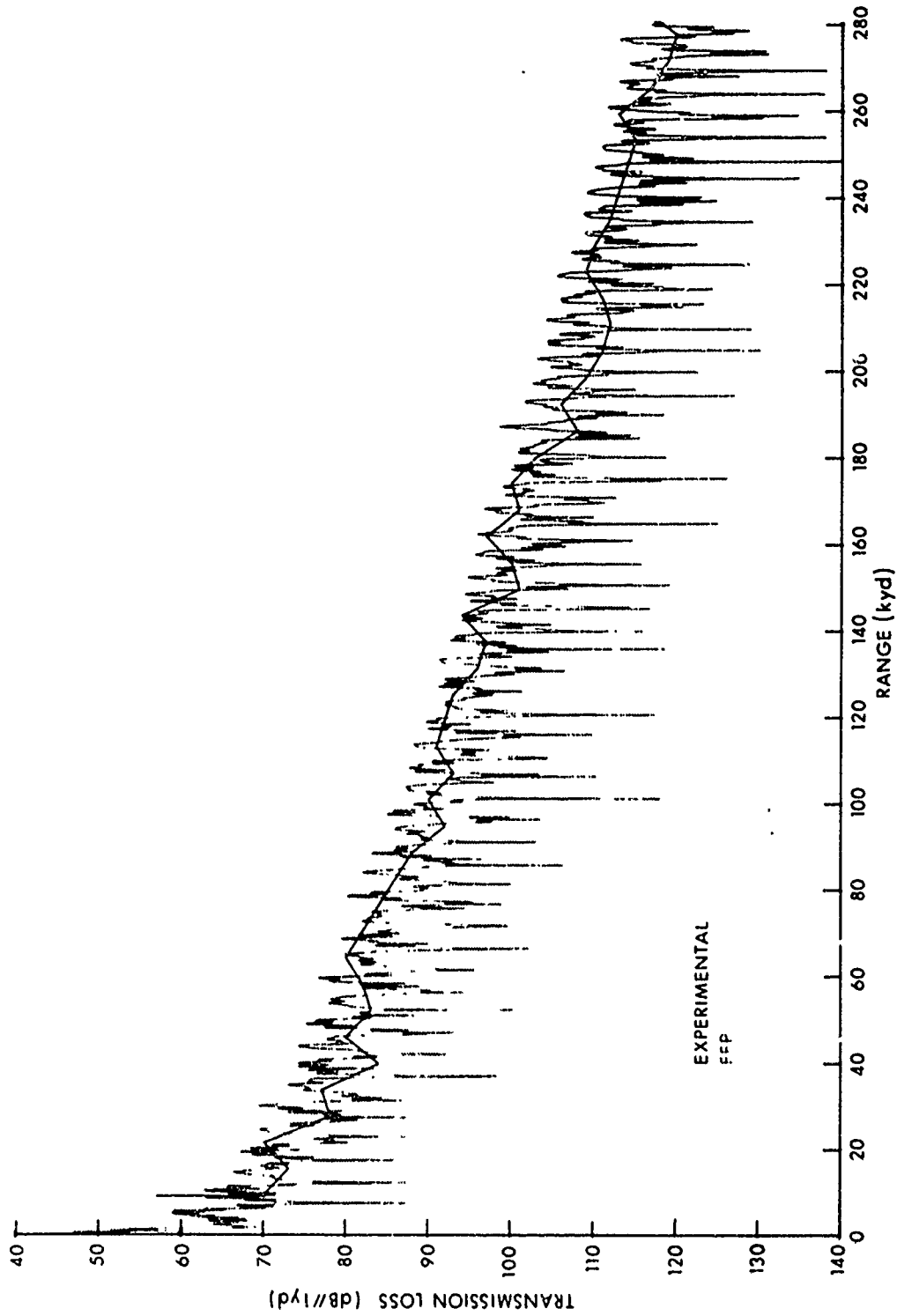
Fig. 18. FFP and Hudson Bay Experimental Transmission Losses at 1250 Hz
(Source Depth 175 ft, Receiver Depth 175 ft, Attenuation 0. 135 dB/kyd)
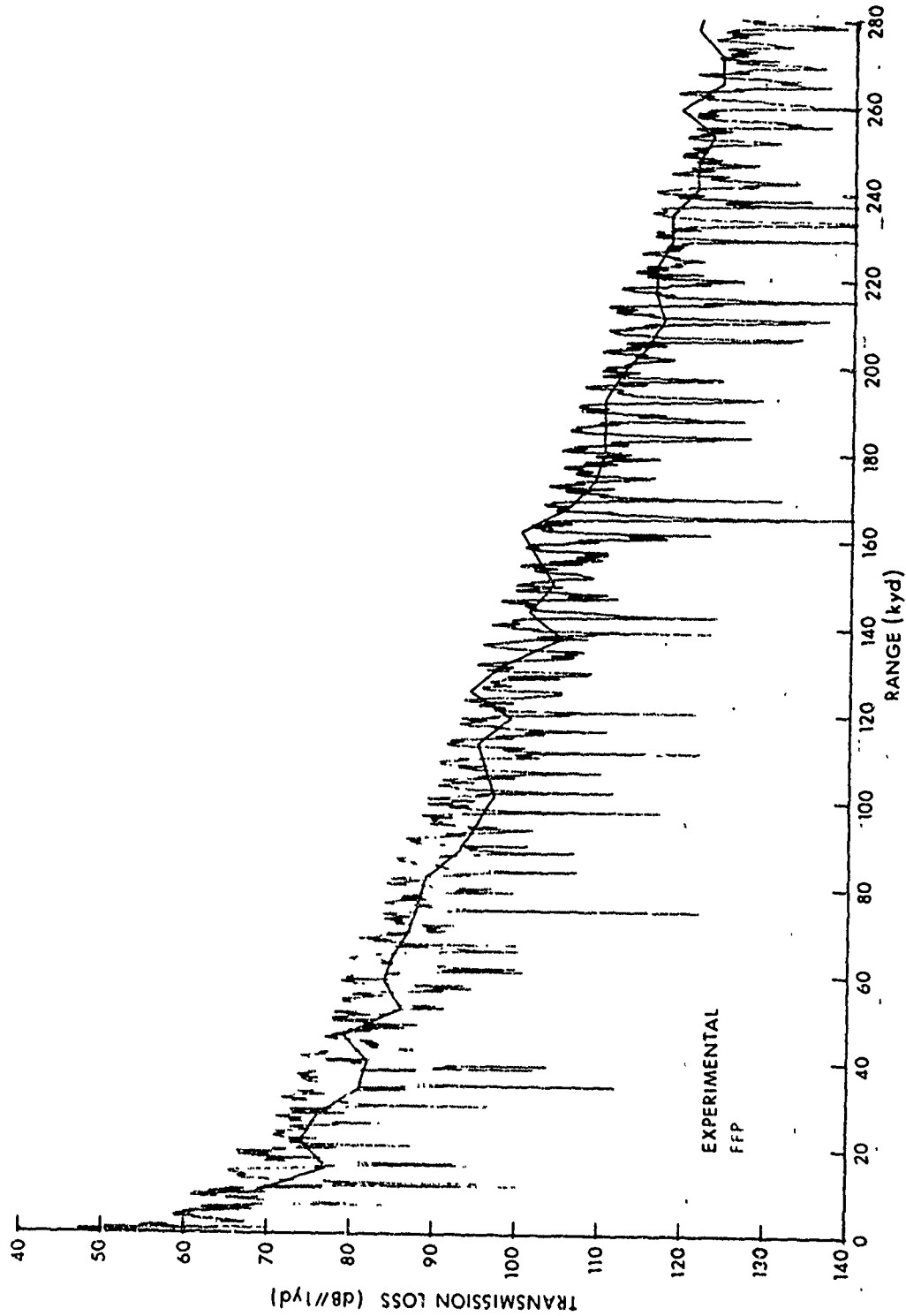
Fig. 19. FFP and Hudson Bay Experimental Transmission Losses at 1600 Hz
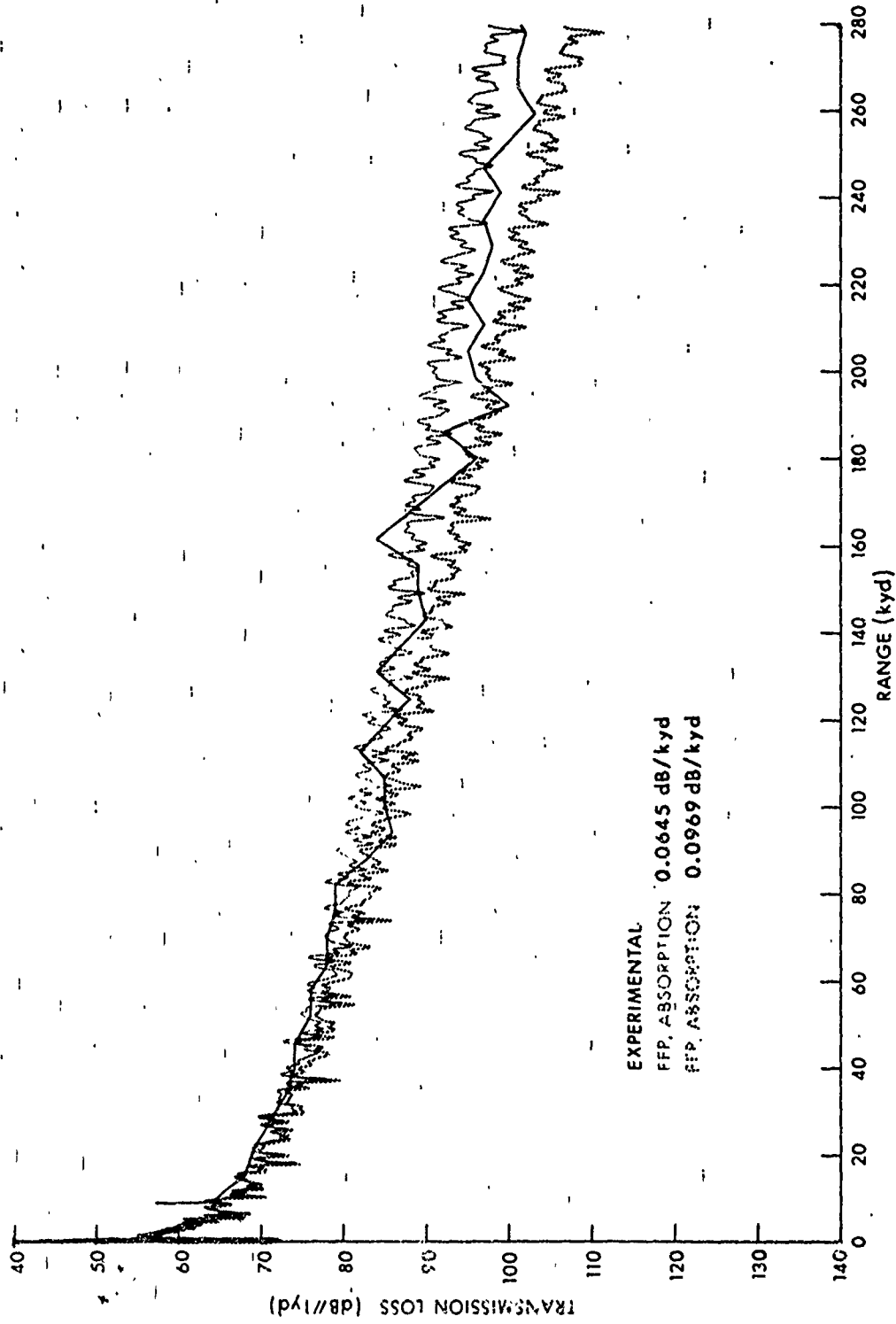(Source Depth 175 ft, Receiver Depth 175 ft, Attenuation 0.170 dB/kyd)

Fig. 20. Example of Uncertainty in Subjectively Determining Attenuation Coefficients
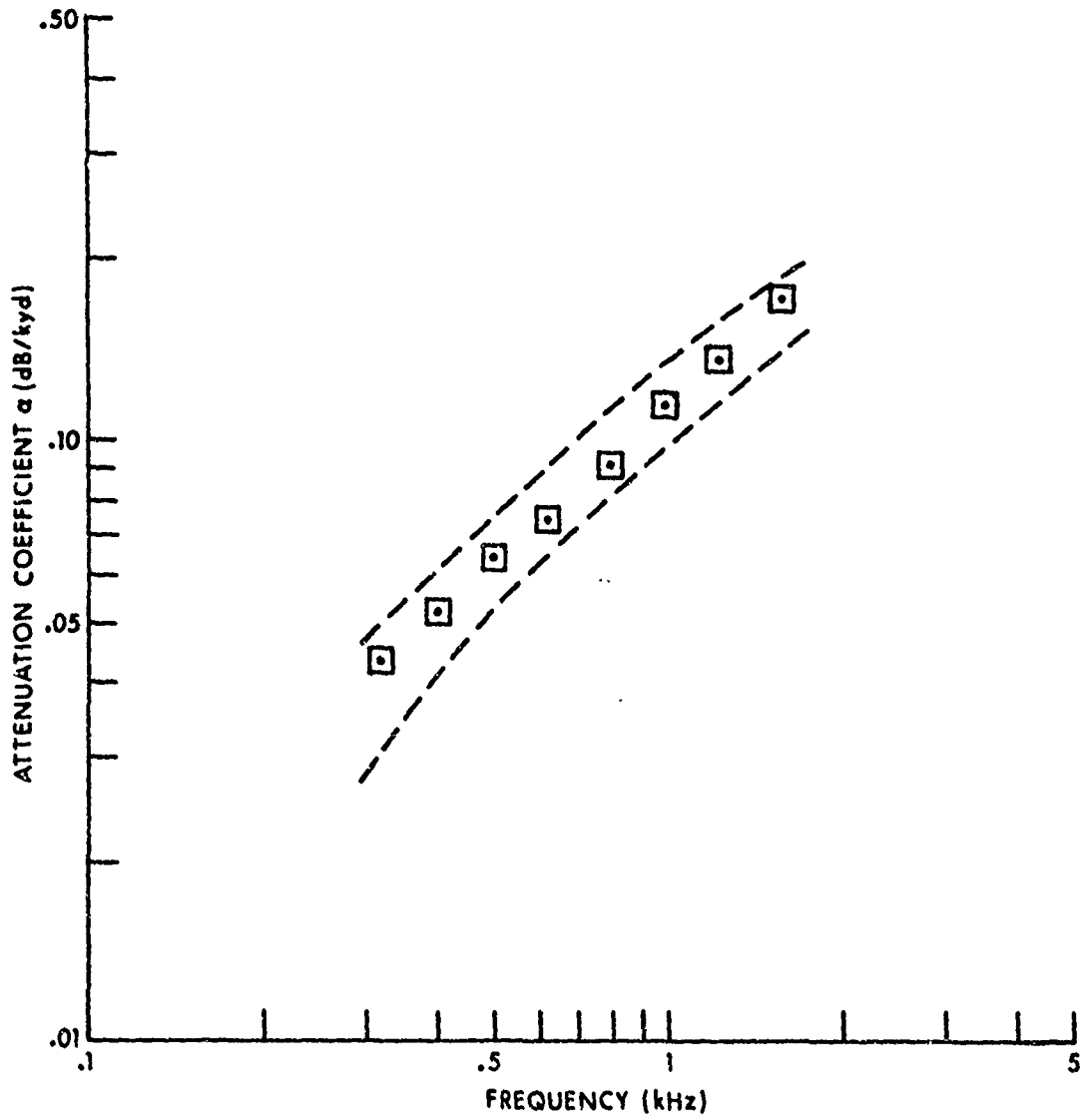(Frequency 630 Hz)

Fig. 21. Limits of Attenuation-Coefficient Input Values Producing
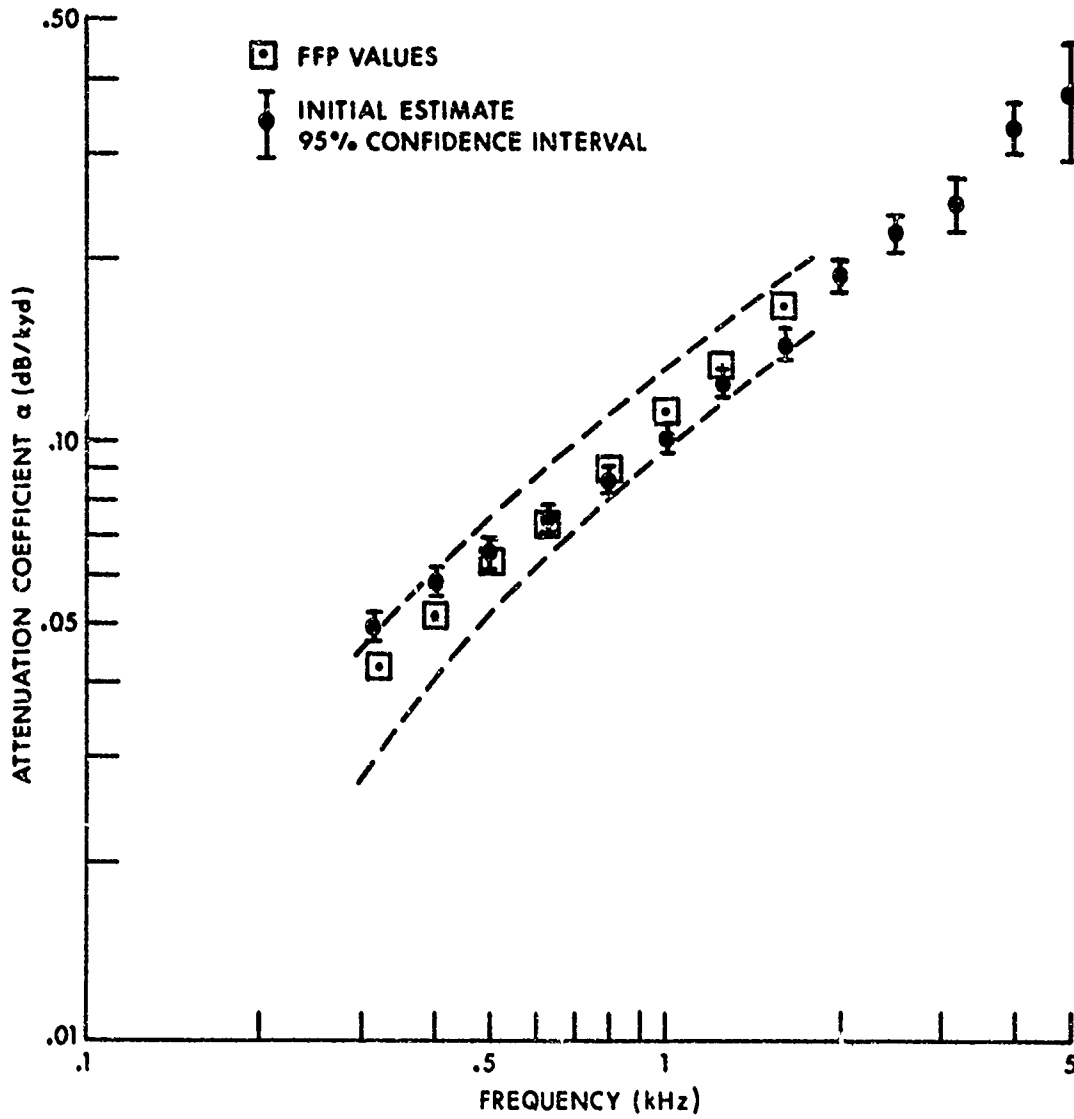Reasonable Comparisons with Experimental Data

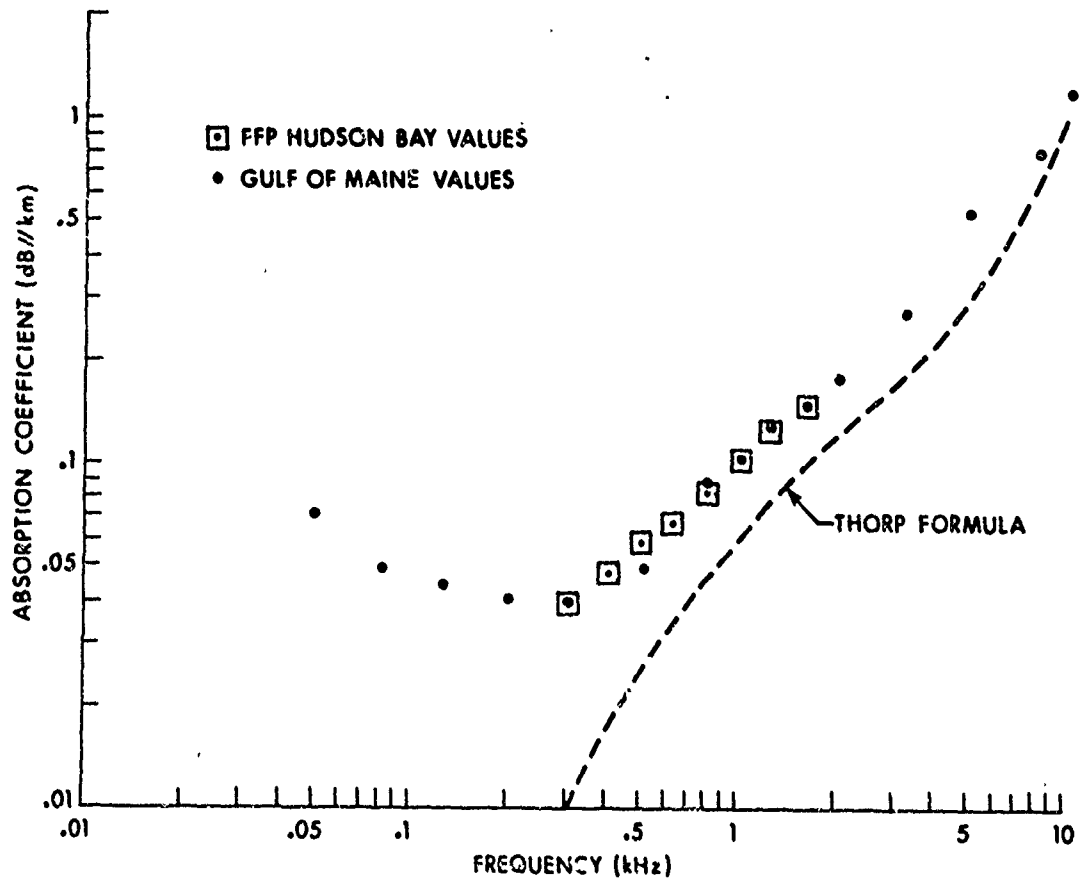Fig. 22. Comparison of Experimental and Analytical Attenuation Values

Fig. 23. Comparison of Attenuation Coefficients
for Hudson Bay and Gulf of Maine

DOCUMENT CONTROL DATA - R & D

Security classification of title, body of abstract and indexing annotation must be entered when the overall report is classified

1. ORIGINATING ACTIVITY (Corporate author)	2a. REPORT SECURITY CLASSIFICATION
Naval Underwater Systems Center Newport, Rhode Island 02840	UNCLASSIFIED
	2b. GROUP

3. REPORT TITLE

THE FAST FIELD PROGRAM (FFP) AND ATTENUATION LOSS IN HUDSON BAY

4. DESCRIPTIVE NOTES (Type of report and inclusive dates)

Research Report

5. AUTHOR(S) (First name, middle initial, last name)

Frederick R. DiNapoli
Mary Rita Powers

6. REPORT DATE	7a. TOTAL NO. OF PAGES	7b. NO. OF REFS
19 April 1972	44	7

8a. CONTRACT OR GRANT NO.	9a. ORIGINATOR'S REPORT NUMBER(S)
b. PROJECT NO. A-670-10 ZF XX 112 001	TR 4253
c.	9b. OTHER REPORT NO(S) (Any other numbers that may be assigned this report)
d.	

10. DISTRIBUTION STATEMENT

Approved for public release; distribution unlimited.

11. SUPPLEMENTARY NOTES	12. SPONSORING MILITARY ACTIVITY
	Department of the Navy

13. ABSTRACT

The Fast Field Program (FFP) was developed to provide rapid, accurate, propagation-loss predictions for a generalized environmental model. This report demonstrates the utility of the FFP, in a different capacity, as a research tool to investigate the sound attenuation in a water column. Hudson Bay was selected as the area of application because the results of propagation experiments conducted there during August 1970 were available and interesting. The experimentally determined values of the attenuation coefficient for the frequency band 315 to 1600 Hz were found to exceed the values that would be predicted from existing formulas based on empirical relationships. The possibility that this anomalous behavior could have been due to energy leakage into the bottom is examined, and the values of the attenuation coefficient determined from the FFP analysis are compared with experimental results.

14 KEY WORDS	LINK A		LINK B		LINK C	
	ROLE	WT	ROLE	WT	ROLE	WT
Attenuation loss						
Low frequency						
Shallow water propagation						

DD FORM 1473 (BACK) (PAGE 2)
1 NOV 65